Millennial slip rates along the eastern Kunlun fault: Implications for the dynamics of intracontinental deformation in Asia

Nathan Harkins[1,*], E. Kirby[1], X. Shi[1], E. Wang[2], D. Burbank[3], and Fan Chun[4]

[1]DEPARTMENT OF GEOSCIENCES, PENNSYLVANIA STATE UNIVERSITY, DEIKE BUILDING, UNIVERSITY PARK, PENNSYLVANIA 16802, USA
[2]INSTITUTE FOR GEOLOGY, CHINESE ACADEMY OF SCIENCES, BEIJING 100864, CHINA
[3]DEPARTMENT OF EARTH SCIENCE, UNIVERSITY OF CALIFORNIA, WEBB HALL, BUILDING 526, SANTA BARBARA, CALIFORNIA 93106, USA
[4]KEY LABORATORY OF MARINE RESERVOIR EVOLUTION AND HYDROCARBON ACCUMULATION MECHANISM, MINISTRY OF EDUCATION, CHINA UNIVERSITY OF GEOSCIENCES (BEIJING), BEIJING 100083, CHINA

ABSTRACT

The role of major strike-slip faults in the Indo-Asian collision zone is central to our understanding of the ways in which continental crust and lithosphere deform in response to continental collision. We investigated how slip varies along the eastern segments of the Kunlun fault in northeastern Tibet. Millennial slip rates were determined based on landforms that are offset by the fault and that were dated using a combination of ^{14}C and cosmogenic radionuclide exposure dating techniques. We developed estimates for slip rates at four new locations along the fault in addition to four previously published sites. All of these sites are located along the eastern 300 km of the fault system, and our results reveal a systematic eastward decrease in slip rate along this portion of the fault since the late Pleistocene. This displacement gradient is consistent with the termination of the Kunlun fault near ~102°E. Coincident variations in fault slip rates and geometry reflect complex kinematics along the fault zone. Although other faults exist in the region, our observations suggest that none of these accomplishes transfer of slip from the primary Kunlun fault system. Instead, we interpret that either the eastern Kunlun fault is relatively young and propagating eastward, or that left-lateral slip is absorbed by interaction of the fault zone with regional rotation of the eastern fault tip. Both of these scenarios contrast with previous interpretations and indicate that the Kunlun fault does not accommodate the eastward extrusion of the central Tibetan Plateau lithosphere.

LITHOSPHERE; v. 2; no. 4; p. 247–266; Data Repository 2010214. doi: 10.1130/L85.1

MOTIVATION

The rates and distribution of slip on Asian strike-slip faults, both ancient and modern, play a central role in conceptual models of the way in which continental lithosphere deforms in response to continental collision. Early recognition of the scale and extent of recent activity along these structures (Tapponnier and Molnar, 1977) led to models that considered eastward displacement of internally rigid blocks of Tibetan lithosphere to be the primary means by which ongoing convergence of India with Eurasia was accommodated (e.g., Molnar and Tapponnier, 1975; Tapponnier et al., 1982). An alternative view, that these faults represent slip along preexisting anisotropy in a continuously deforming medium, arose out of considerations of the strength of common constituents of continental lithosphere and the forces generated during crustal thickening (e.g., England and McKenzie, 1982; Houseman and England, 1993).

This debate has stimulated numerous investigations into displacement rates along active faults in Asia, including the Altyn Tagh (e.g., Cowgill, 2007; Gold et al., 2009; Mériaux et al., 2004, 2005; Zhang and Molnar, 2007), Haiyuan (e.g., Lasserre et al., 2002, 1999; Ruddiman and Kutzbach, 1989; Zhang et al., 1990), Kunlun (e.g., Li et al., 2005; Van der Woerd et al., 2000, 2002b), and Karakorum faults (e.g., Brown et al., 2002; Chevalier et al., 2005) (Fig. 1). The results of these studies have implications for whether recent displacement represents a large or small fraction of the total convergence rate between India and Eurasia. Other works help to constrain the total amount of displacement and long-term kinematic histories of these structures (e.g., Cowgill et al., 2004; Fu and Awata, 2007; Kidd and Molnar, 1988; Murphy et al., 2000; Robinson, 2009; Yin and Harrison, 2000), and therefore have similar implications for the role of these fault zones in the long-term tectonic evolution of the Tibetan Plateau. The relatively low total displacements and slow displacement rates interpreted along Tibetan strike-slip faults by the majority of these studies favor the continuum models of plateau deformation. Despite these findings, however, and the coincidental advent of geodetic technologies to measure rates of interseismic deformation, recent geodynamic modeling has shown that these rates can still be placed within a block displacement framework (cf. Meade, 2007; Thatcher, 2007; Wang et al., 2001; Zhang et al., 2004). Thus, fundamental differences between these views of active deformation in Eurasia still exist.

The nature of deformation at or near a fault tip is sensitive to both the bulk rheologic properties of the crust (e.g., Barr and Houseman, 1996) and to the external forces driving fault slip (e.g., Burchfiel et al., 2008). As a result, a kinematic and mechanical analysis of the way in which a major fault zone terminates within the Tibetan Plateau may carry additional, unique constraints on the mechanical properties of the associated lithosphere. Major faults such as the Altyn Tagh and Haiyuan faults separate actively deforming regions of the Tibetan Plateau from its undeformed foreland, and thus the termination of these structures is easily understood by displacement transfer into regions of active shortening in the Qilian Shan and Liupan Shan, respectively (Burchfiel et al., 1989; Tapponnier et al., 1990; Zhang et al., 1990). The Kunlun fault, another major Tibetan strike-slip fault zone, is somewhat distinct from these other fault zones

*Present address: ExxonMobil Upstream Research Company, 3120 Buffalo Speedway, Houston TX 77098.

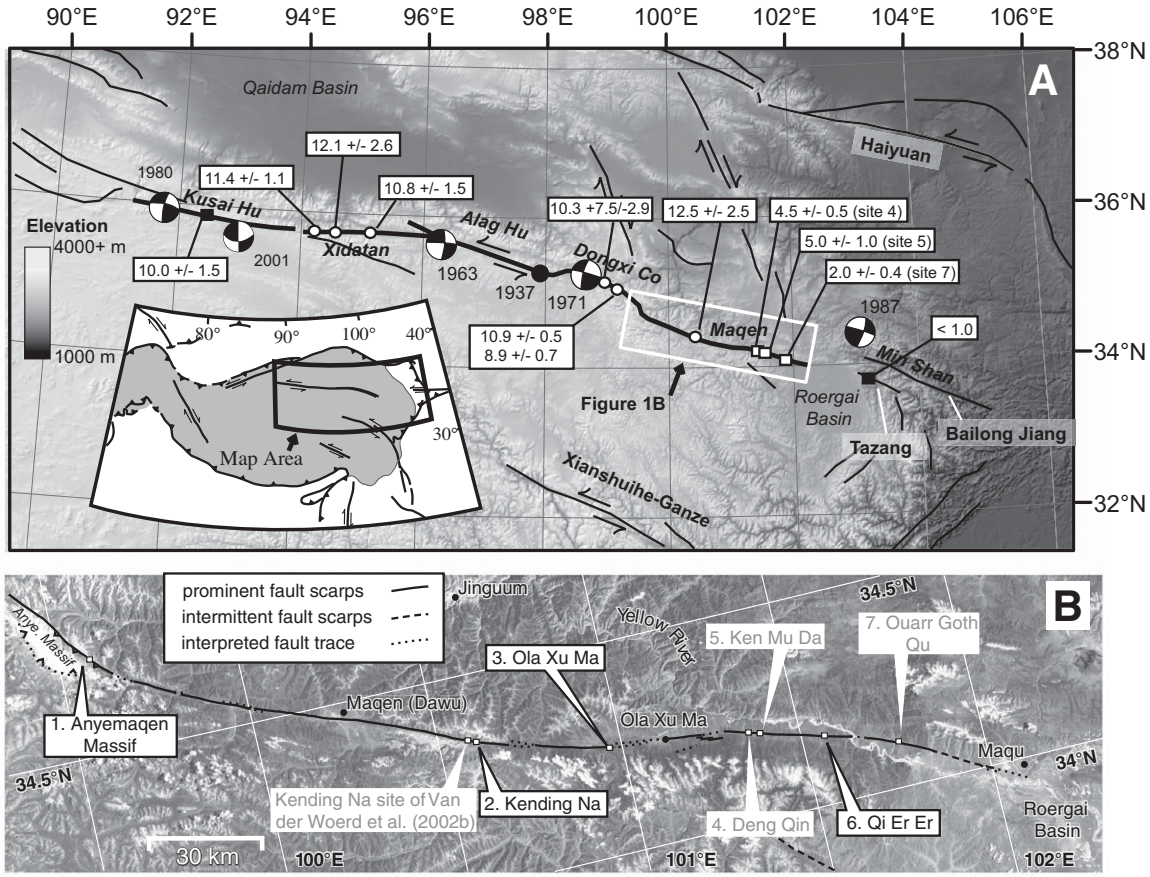

Figure 1. (A) Shaded relief map of the northern Tibetan Plateau with some of the major strike-slip faults labeled. The Kunlun fault is highlighted in bold, and millennial slip rates from previous works are shown. White circles are from Van der Woerd et al. (2002b), black box is from Li et al. (2005), and white boxes are from Kirby et al. (2007). Fault segments are labeled in bold italics. Epicentral locations and focal mechanisms of recent seismicity along the Kunlun fault are compiled from U.S. Geological Survey (USGS; http://earthquake.usgs.gov/earthquakes/eqarchives/epic/), Harvard Centroid Mean Tensor (CMT) catalog (http://www.globalcmt.org/CMTsearch.html), and Molnar and Lyon-Caen (1989). Index map displays all of Tibet, shaded regions are above 2000 m in elevation, and area covered by Figure 1A is shown. (B) Landsat mosaic of the easternmost Kunlun fault. Geomorphic character of the fault is highlighted, along with the locations of the eight slip-rate sites discussed in the text. The four new sites presented in this work (sites 1, 2, 3, and 6) are labeled in black with outlined boxes, and previously published sites are labeled in gray.

because it is embedded within actively deforming regions of the Tibetan Plateau. In the west, the fault terminates in a series of active N-S–striking normal faults and NW-striking thrusts in the Qimen Tagh range (e.g., Yin, 2000; Yin et al., 2007). Indeed, Yin (2000) cited these and other normal faults in a discussion on the strength of the Tibetan lithosphere and geodynamic architecture of extension in the central Tibetan Plateau. The eastern termination of the Kunlun fault, however, lacks obvious evidence of similar accommodation features and has therefore been interpreted under a variety of geodynamic models.

Spatially uniform slip rates along the central ~600 km of the fault system (e.g., Van der Woerd et al., 2000, 2002b) have been cited as evidence that this fault system accomplishes eastward extrusion of Tibetan lithosphere via linked structures in the Qilian Shan (e.g., Peltzer et al., 1985; Van der Woerd et al., 2002b). However, recent studies of slip rates along the eastern ~200 km of the Kunlun fault suggest that rates decrease systematically to less than ~1 mm/yr, challenging the assumption of a continuous fault system across the eastern margin of the Tibetan Plateau (Harkins and Kirby, 2008; Kirby et al., 2007).

In this paper, we evaluate the hypothesis of Kirby et al. (2007) that the fault terminates within the plateau. We utilized displaced geomorphic features at four new localities along the easternmost segments of the Kunlun fault to determine slip rates. Our additional chronology allows us to bolster the interpretations at sites previously published by Kirby et al. (2007) and Harkins and Kirby (2008). Collectively, our results confirm the presence of a displacement rate gradient near the eastern fault tip and refine the shape of this gradient. Observations on other faults in the region suggest that these structures do not transfer significant displacement away from the primary Kunlun fault system. Importantly, the magnitude of the gradient (the change in slip rate over a strike distance) and any along-strike changes in this gradient may provide additional constraints on the mechanical properties of the lithosphere. Thus, the characteristics of recent strain along the easternmost Kunlun fault, whether it is transferred beyond the plateau margin or is absorbed within the plateau itself, and the ways in which either of these behaviors are mechanically accommodated are two parts of a growing quantitative description of active deformation within the Tibetan Plateau.

BACKGROUND AND APPROACH

The Kunlun fault system extends E-W across ~1200 km of the northern Tibetan Plateau between 34°N and 36°N latitude (Fig. 1). The western portions of the fault system occur in the high ranges that mark the southern boundary of the Qiadam Basin, whereas the eastern portions of the fault system follow the Anyemaqen suture, a major lithospheric boundary that marks the northern extent of the Songpan-Garzi terrane (e.g., Zhou and Graham, 1996), and extend into the high topography of the Anyemaqen Shan. Because the Kunlun fault is parallel to primary ancient geologic structures, little is known about the total displacement. A recent study by Fu and Awata (2007) correlated Jurassic plutons and suggested that displacement may be on the order of ~100 km, although the portion of this that is Cenozoic in age remains an open question. Likewise, the onset timing of left-lateral faulting along the Kunlun fault is uncertain. The best estimate derives from the age of volcanism and associated extensional deformation near 90°E at ca. 15 Ma (Jolivet et al., 2003).

Significantly more information is available for the rate of slip along the Kunlun fault during Quaternary time. Kidd and Molnar (1988) first suggested that the Quaternary slip rate along the central (Xidatan) segment of the fault was on the order of 10–15 mm/yr, based on the provenance of moraines that had been displaced left-laterally. In a seminal study, Van der Woerd and colleagues determined slip rates at six sites along the central ~600 km of the fault system, and determined that slip rates were relatively uniform at 10–12 mm/yr (Van der Woerd et al., 1998, 2000, 2002b). Li et al. (2005) determined slip rates along the Kunlun fault farther west, such that slip rates during the late Pleistocene and Holocene appear to be spatially uniform along the Kunlun fault between ~92°E and ~101°E. In contrast, as noted above, slip rates along the eastern segments of the fault system (between ~101°E and ~103°E) appear to decrease systematically from >5 mm/yr to <1 mm/yr.

The central and western segments of the Kunlun fault have experienced several large-magnitude seismic events that produced left-lateral surface ruptures in the twentieth century (Fig. 1). Events in 1937 and 1963 (at ~98°E and 96.5°E, respectively) in the Dongxi Co and Alag Hu segments were estimated to have M_w ~7.0 and resulted in over 100 km of along-strike rupture extent each (Fitch, 1970; Li and Jia, 1981). A M_w = 6.4 event in 1971 at ~98.6°E, also in the Dongxi Co segment, did not produce a surface rupture, but represents the easternmost large event that has been recorded along the Kunlun fault (Tapponnier and Molnar, 1977). A M_w = 7.6 event in 1997 (epicenter at ~35.1°N, 87.3°E) produced an ~170 km strike length of surface rupture along the Manyi fault (Peltzer et al., 1999), an E-W–striking fault zone to the south and west of the main trace of the Kunlun fault. Most recently, the M_w = 7.8 Kokoxili event in 2001 ruptured over 400 km of strike length between ~90°E to 95°E along the westernmost segments of the Kunlun fault (Lasserre et al., 2005). The locations of these events highlight a sharp contrast between the central extent of the Kunlun fault and eastern extent between ~101°E and ~103°E, where there is no historic seismicity. Recent investigations of the paleoseismic record along this segment of the fault (Lin and Guo, 2008) suggest that the most recent event occurred ca. 1500 ka, consistent with a relatively slow slip rate (~3 mm/yr).

Determining Slip Rates from Displaced Geomorphic Markers

In this study, we utilized geomorphic features as markers of displacement along the Kunlun fault, including both glacial moraines and fluvial terraces. Each of these markers is subject to a suite of uncertainties that reflect the dynamic evolution of the landforms in response to continuing erosion, and the manner in which these changes impact the various chronologic systems that are used to date the landforms themselves.

Where the Kunlun fault crosses high topography in the Anyemaqen Shan, recent advances of glaciers deposited a series of sublinear moraines across the trace of the fault that allow fairly precise reconstruction of fault slip. Establishing age control for these moraines, however, is a difficult task, and we follow an extensive body of work that employs exposure dating of large (>1-m-diameter) boulders atop moraine crests based on accumulations of cosmogenic radionuclides (CRN) (e.g., Gosse and Phillips, 2001; Owen et al., 2003; Phillips et al., 1997), specifically ^{10}Be. These methods are subject to uncertainties that arise from the degradation of the moraine and from weathering of the boulders themselves (e.g., Putkonen and O'Neal, 2006), as well as uncertainties in the initial distribution of isotope concentrations (typically referred to as "inheritance"). Consequently, the interpretation of the age of a moraine from a distribution of individual exposure ages can lead to widely varying slip-rate estimates (cf. Brown et al., 2002; Chevalier et al., 2005). In this study, we adopted a relatively conservative approach of taking the maximum and minimum ages from the distribution as a measure of the range of allowable ages, and thus slip rates. All samples were subjected to preprocessing at either the (former) Dartmouth College CRN laboratory or the Purdue Rare Isotopes Measurement (PRIME) laboratory that included separation of pure quartz, extraction of ^{10}Be, and preparation of accelerator mass spectroscopy (AMS) targets. AMS analysis of all samples was conducted at the PRIME laboratory.

Fluvial terrace risers provide a particularly useful marker for reconstructing lateral slip along a fault because the intersection between the terrace tread and riser provides a linear marker (e.g., Lensen, 1964a, 1964b), and terrace treads typically incorporate datable material, such as detrital charcoal. However, the relationship of ages from a terrace tread to the "age" of the riser that separates them is inherently uncertain and depends on a set of assumptions about the degree of lateral erosion by an incising stream. Although most workers have simply assumed that the riser is actively undercut by the stream until abandonment of the lower bounding terrace tread (e.g., Berryman, 1993; Bull, 1991; Grapes et al., 1993; Knuepher et al., 1987; Mériaux et al., 2004, 2005; Van der Woerd et al., 1998, 2002b), recent work has shown that this is not always a reasonable assumption (Cowgill, 2007) and that significant slip can accrue during occupation of the lower tread (e.g., Harkins and Kirby, 2008). Thus, we take a more conservative approach to assigning slip rates that considers the upper and lower terrace tread ages as maximum and minimum bounds on the age of the riser (e.g., Kirby et al., 2007; Zhang et al., 1990).

Chronology of Late Pleistocene Deposits along the Kunlun Fault

Copious amounts of existing data on the timing of terrace formation at locations along the eastern Kunlun fault (e.g., Harkins and Kirby, 2008; Kirby et al., 2007; Van der Woerd et al., 2002b), as well as a study of glacial moraines in the Anyemaqen Shan (Owen et al., 2003), provide a chronostratigraphic framework for late Pleistocene through Holocene alluvial and glacial deposits in our study area. As recognized by Van der Woerd et al. (2002b), these deposits cluster in age and likely reflect a profound climatic control on the synchronicity of fluvial incision and deposition in northern Tibet. Here, we briefly review these data to establish a foundation for our new chronology at sites along the eastern Kunlun fault.

Along the central Kunlun fault, most of the terraces dated by Van der Woerd et al. (1998, 2000, 2002b) were formed between ca. 5 ka and 13 ka and postdate the warming that occurred following the Last Glacial Maximum (LGM) (Thompson et al., 1997). This time period is coincident with slightly increased precipitation in northern Tibet that appears to have been responsible for variations in fluvial incision (Poisson and Avouac, 2004). Terraces younger than 5 ka are rare and may reflect increasing aridity during the late Holocene (Gasse et al., 1991). Likewise, older alluvial deposits

are rare along the central Kunlun fault and are apparently confined to the Dongxi Co segment (Fig. 1A) (Van der Woerd et al., 2002b).

This basic chronology appears to exist along the eastern Kunlun fault as well, where fluvial incision along the Yellow River has sustained relative base-level fall along tributaries that cross the eastern segments of the fault system between Dawu and Maqu (Fig. 1) (Harkins et al., 2007; Kirby et al., 2007). In this region, the oldest deposits occur as a broad fan-terrace complex that appears to be a relict piedmont surface. Radiocarbon ages from overlying loess deposits constrain this alluvial deposit to be older than ca. 22–28 ka in age, consistent with development during the LGM. Fluvial incision appears to have initiated by ca. 15 ka and was responsible for abandonment of the highest terraces observed along the eastern Kunlun fault. Subsequent terrace formation and abandonment appear to have occurred between 9 and 10 ka, 7 and 9 ka, and 5 and 7 ka. Similar to western sites, few terraces younger than 5 ka are present.

Glacial advances in the Anyemaqen Shan reflect similar variations in climate. Based on cosmogenic radionuclide (CRN) concentrations in boulders on moraines located on the northeastern side of the massif, Owen et al. (2003) determined that the most recent glacial advance (termed the Hailong glacial by these authors) occurred at 9 ± 3 ka. Older moraines record advances between 10 and 20 ka (Qiemuqu glacial) and between 30 and 50 ka (Anyemaqen glacial). A single moraine along the Kunlun fault, east of Dawu (at the Kending Na site; Fig. 1), was constrained by Van der Woerd (2002b) and others to be older than 12 ka, consistent with either glacial advance.

Slip Rates along the Eastern Kunlun Fault

The regional chronology places direct constraints on the ages of deformed landforms used to constrain slip rates along the eastern segment of the Kunlun fault. Previous work has been conducted at four sites along the trace of the fault, and at one site along structures farther east (Fig. 1). The westernmost of these sites, described as the Kending Na locality by Van der Woerd et al. (2002b), preserves a moraine ridge that is offset across the trace of the Kunlun fault. These authors interpreted an approximate moraine age of ca. 12 ka to estimate a maximum slip rate of 12.5 ± 2.5 m/k.y. at this site. Approximately 75 km east of Kending Na, two sites are proximally spaced to one another along adjacent tributaries of the Yellow River, locally referred to as Deng Qin and Ken Mu Da (Fig. 2A) (Kirby et al., 2007). Both of these channel valleys preserve a suite of fluvial terraces characterized by risers that are progressively displaced along the Kunlun fault (Figs. 2B and 2C). Terraces at both of these sites are strath terraces that are all cut into the old, relict piedmont surface described in the previous section. Progressive offset of the risers between the T1 through T4 surfaces records left-lateral geologic slip rates of 2.7–9.7 m/k.y. at Deng Qin, and 4–6 m/k.y. at Ken Mu Da since the latest Pleistocene. Harkins and Kirby (2008) used a calibrated scarp degradation model to more tightly constrain riser ages at Deng Qin, and they argued for a narrower the range of allowable slip rates at this site of 3.7–7.3 m/k.y. It is worth emphasizing the similarity in both ages of terraces between sites (Fig. 2E), and that the ages independently yield similar results for the slip rate.

At the easternmost site described by Kirby et al. (2007), located where the fault crosses the Ouarr Goth Qu (river), a flight of three extensive terrace surfaces (T1–T3) is preserved on the east side of the channel (Fig. 2D). Here, again, these terraces are straths cut into a relict piedmont surface of the same age as that described at Ken Mu Da and Deng Qin. All terraces are underlain by, and cut into, well-indurated gravels with similar characteristics to the strath gravels described at Deng Qin and Ken Mu Da. A single well-preserved offset of the local T2/T3 riser records a maximum range of slip rates of 1.6–2.4 m/k.y. at this site since ca. 10 ka. Kirby et al. (2007) also investigated terraces formed across the Tazang fault (Fig. 1), a potentially active structure along the eastern margin of the Roergai Basin that has been suggested to be an extension of the Kunlun fault (Van der Woerd et al., 2002b). Terraces as old as ca. 9 ka are not displaced by the Tazang fault, and thus slip rates here are likely <1 mm/yr.

Overall, slip rates along the eastern Kunlun fault appear to decrease systematically from west to east between ~100.5°E and 103°E. Importantly, this decrease in slip rate is apparent in modern geodetic data (Zhang et al., 2004), where the component of velocity parallel to the Kunlun fault also decreases toward the east (cf. Kirby et al., 2007). We view the Deng Qin and Ken Mu Da sites together as a single well-described slip-rate determination due to their the spatial proximity and similar slip rate. Therefore, slip rates are presently described at effectively only three locations along the eastern segment of the Kunlun fault. Moreover, in order to consider the regional geodynamic implications of slip rates along the Kunlun fault, the fact that any one site may record only some fraction of the total displacement budget across the entire Kunlun fault zone must be addressed. As a result, our primary goal in the research that follows is to present additional data from four new slip-rate sites along this same segment of the Kunlun fault that confirm this slip-rate gradient and refine the extent over which displacement decreases at the eastern tip of the fault. The new slip-rate determinations are at the Anyemaqen Massif, East Kending Na, Ola Xu Ma, and Qi Er Er sites. We also provide additional, previously unpublished geochronologic data on the ages of offset terraces at the Ken Mu Da site described in Kirby et al. (2007) and Harkins and Kirby (2008). Finally, we discuss observations from other structures in the region that may interact with the Kunlun and consider some of the mechanical implications of our results.

NEW SLIP-RATE SITES

Anyemaqen Massif

The Kunlun fault passes through a restraining bend between 99.2°E and 99.6°E, resulting in local contraction that is responsible for the high topography of Anyemaqen Massif. The most obvious active strand of the Kunlun fault occupies the valley that skirts the northern side of the massif, although some authors (e.g., Van der Woerd et al., 2002b) interpret an additional active strand of the Kunlun on the south side of the massif. The massif hosts a modern ice cap, and it has provided the source area for late Pleistocene and Holocene glaciers that deposited extensive moraine complexes across the trace of the Kunlun fault (Owen et al., 2003). We studied moraines in a small catchment located at ~99.6°E, along the eastern edge of the massif (Fig. 3A). To reconstruct displacement of these features, we conducted a topographic survey using a differential Global Positioning System (GPS) system and mapped individual moraine crests atop this topographic base (Fig. 3C). We augmented these data with color satellite imagery (Quickbird platform, Fig. 3B) of these moraines and collected samples of moraine boulders for cosmogenic nuclide exposure age analysis.

Moraines at this site consist of a nested series of lateral moraines of relatively subdued relief that appear to have been deposited on the northwestern margin of the glacier (supplemental Fig. DR1).[1] The geometry of the preserved moraines suggests that the glacier flowed northeast from its accumulation zone high in the massif and turned abruptly to the southeast when it reached the valley hosting the Kunlun fault. The fault

[1]GSA Data Repository Item 2010214, Figures DR1–DR11, is available at www.geosociety.org/pubs/ft2010.htm, or on request from editing@geosociety.org, Documents Secretary, GSA, P.O. Box 9140, Boulder, CO 80301-9140, USA.

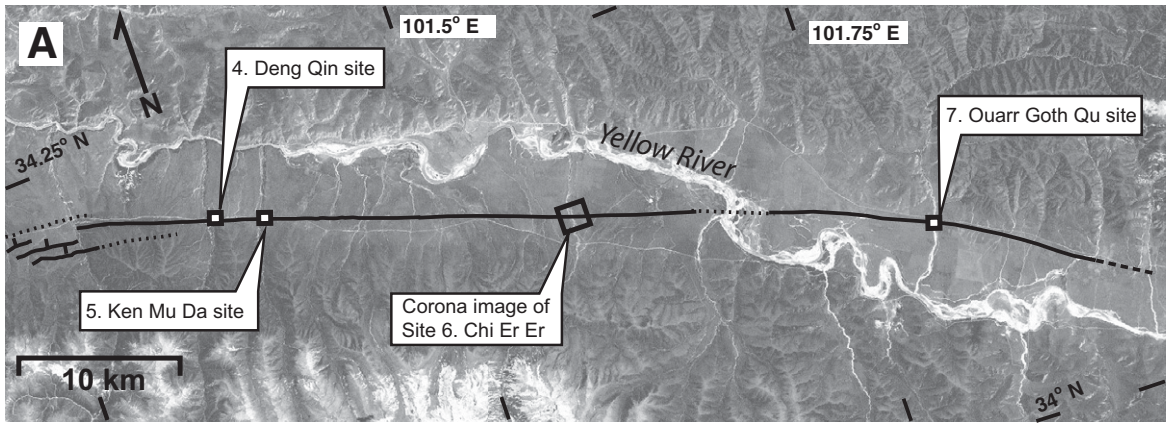

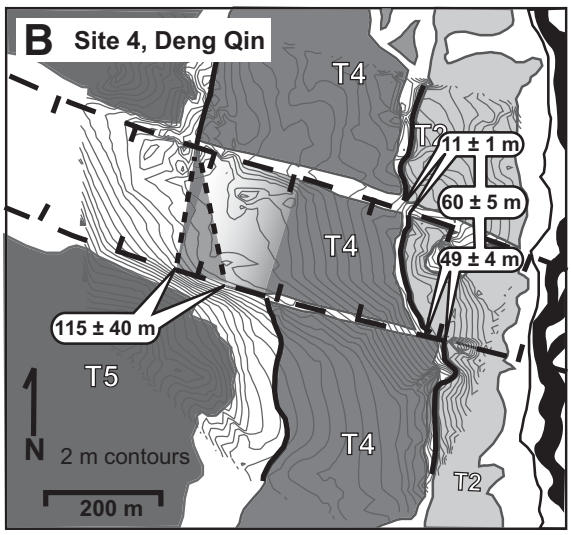

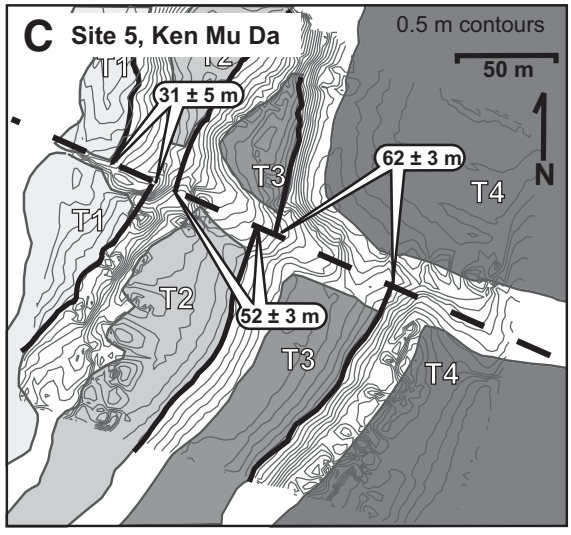

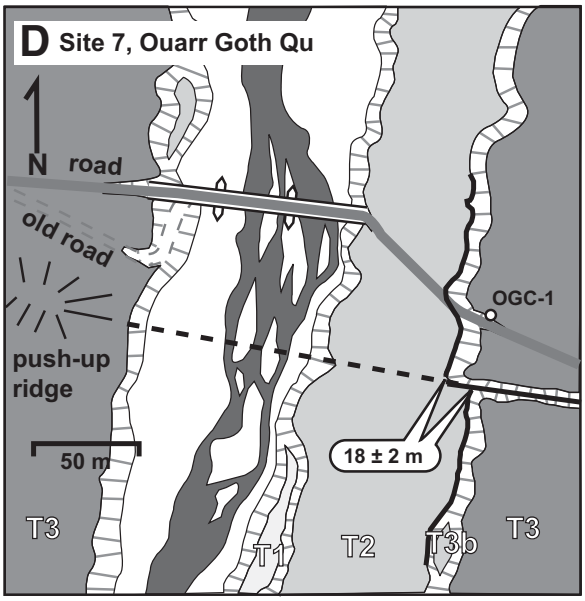

E Fluvial Terrace Chronostratigraphy

Event	~ Age	Site & Terrace 4	5	7
Middle Holocene II	ca. 5-6 ka	-	T1*	-
Middle Holocene I	ca. 6-7ka	T2	T2	T1*
Early Holocene	ca. 9-10.6 ka	T3	T3*	T2*
Late Pleistocene	ca.14-15 ka	T4*	T4*	T3

*** denotes terraces with direct ^{14}C age control**

Figure 2. (A) Landsat image of the portion of the Kunlun fault hosting the Deng Qin, Ken Mu Da, and Ouarr Goth Qu sites as well as the Qi Er Er site (discussed later in the text). (B–C) Interpreted maps of offset terraces and risers from Deng Qin (left) and Ken Mu Da (right). Topographic base maps are constructed from kinematic Global Positioning System (GPS) surveys of sites. Surveyed riser toes are highlighted in bold; offsets of these risers are labeled. Sample locations are delineated. (D) Interpreted map of offset risers at the Ouarr Goth Qu site. Slip-rate determinations at the Deng Qin, Ken Mu Da, and Ouarr Goth Qu sites have been previously published in Kirby et al. (2007) and Harkins and Kirby (2008). (E) Correlation chart of terrace abandonment ages between the three sites.

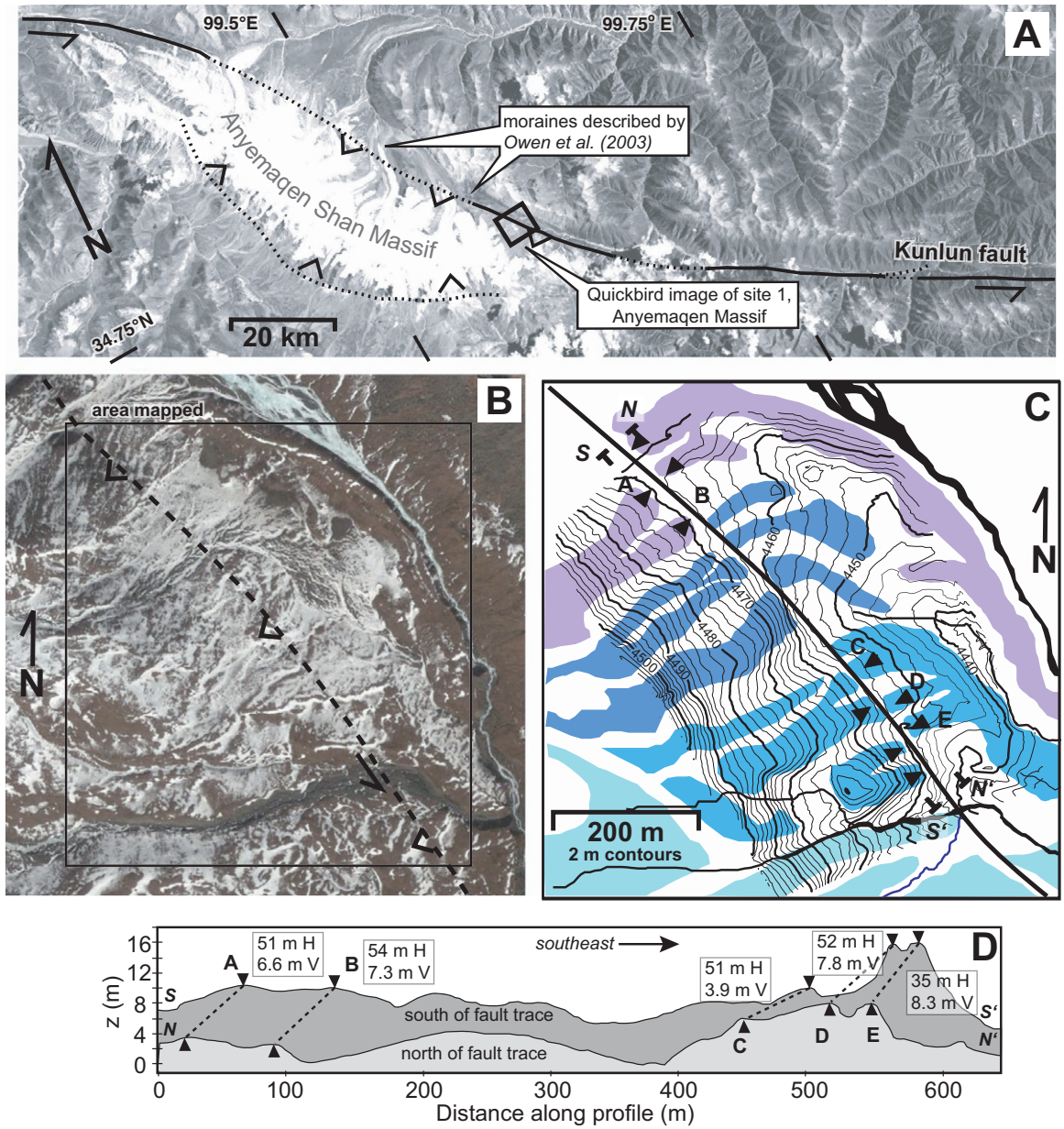

Figure 3. (A) Landsat image of the portion of the Kunlun fault near the Anyemaqen Massif. Location of the Anyemaqen Massif slip-rate site is delineated. (B–C) Quickbird satellite image and interpreted map of offset moraines at the Anyemaqen Massif site. Interpreted map is drawn over a topographic base compiled from a kinematic Global Positioning System (GPS) survey of the site. Piercing points at moraine crests are highlighted by the black triangles and assigned letters. These letters correspond to the labels on topographic profiles. (D) Along-strike topographic profiles immediately north and south of the fault trace (profile end points are labeled on the interpreted map). Moraine crest offsets are displayed along with associated horizontal and vertical offsets.

itself follows a single trace through the northeast-trending moraines and forms a series of north-facing scarps. The gently curving map trace of the fault over topography suggests a relatively steep (>60°) fault dip to the southwest. Although much of the survey area has been modified by postdepositional fluvial erosion, several moraine ridges are preserved well enough to facilitate reconstruction of fault slip. Intact moraines are mantled with up to 1 m of loess, and sporadic meter-sized boulders protrude through the loess cover. A steep, tall (>20 m), and boulder-rich moraine that lacks a loess mantle is located ~600 m southwest (up valley) from the survey area and is apparently much younger than the surveyed moraines. This moraine does not cross the Kunlun fault, however, and we did not investigate it further.

Within the survey area, moraine crests are consistently displaced in a left-lateral sense across the trace of the fault. Individual crests of moraine ridges were mapped in the field and subsequently identified on a topographic base developed from a differential GPS survey. Transects parallel to the fault reveal five moraine crests that can be matched across the fault based on their height and position (Fig. 3D). Horizontal offsets measured from four moraine crests cluster tightly between 51 and 54 m, while a fifth reconstruction yields a somewhat lower value of 35 m. The latter value

is based on the offset of a moraine that is directly adjacent to an actively eroding stream channel. Lateral erosion of the stream has likely modified the morphology of this moraine ridge on the SW side of the fault, resulting in a lower magnitude of apparent offset in this particular feature. As a result, we consider the 51–54 m reconstruction to be more representative of actual fault displacement since moraine deposition.

The fault trace is marked by 10–20 m of disrupted till, imparting a degree of uncertainty in offset determinations from the projection of moraine ridge crests across this zone. To account for this uncertainty, we derived a full range of allowable crest positions for each moraine ridge given 0.5 m of observed surface roughness. Under this treatment, we considered any position on a moraine crest within 0.5 m of the mapped crest elevation to be allowable. This approach expanded the range of allowable offsets to 45–59 m.

The fault at this site appears to have a systematic component of south-side-up displacement. Although all moraine crests are higher on the south side of the fault, the hummocky topography along the moraine crest imparts significant uncertainty in the projection of moraine crests. As a result, we estimated vertical displacement by taking the elevation difference between points on intact moraine crests directly adjacent to either side of the fault zone. Since all moraine crests exhibit a net slope to the northeast (across the fault zone), the reported vertical offsets of 3.9–8.3 m are likely overestimates of actual vertical offset magnitudes. Preserved scarps in adjacent moraine troughs are ~3–4 m in height, suggesting that vertical offset since the time of moraine deposition is actually of that magnitude.

Moraine Ages and Slip Rates

We sampled the largest protruding boulders on moraine crests for CRN exposure age determination (Table 1). All boulders are composed of a silicic metaconglomerate that is rich in quartz. We sampled only boulders of sufficient height (>1 m) to minimize the possibility of burial during eolian deposition of loess (supplemental Fig. DR2 [see footnote 1]). Unfortunately, boulders of this size are rare, and we were only able to sample eight individual boulders.

Of these eight samples, four yielded ages that cluster between 7.9 and 9.3 ka (ca. 8 ka), three samples returned younger ages (between 2.5 and 5 ka), and a single sample returned a much older age of 15 ± 1.5 ka. This range of sample ages does not exhibit any consistent age differences between separate moraine crests in our survey area. However, two of the samples with ages younger than 5 ka were extracted from the smallest boulders in our study area, suggesting the possibility that these boulders may have been buried and subsequently exhumed since deposition. We think this is a reasonable explanation for these young ages, given that regional studies (e.g., Owen et al., 2003) suggest that glaciers in northeastern Tibet were retreating throughout the middle and late Holocene. We are unable, with the sparse sample set available, to discern whether exhumation may have influenced our other samples as well. It is possible that our oldest sample is most reflective of the age of deposition at ca. 15 ka. However, we think that the cluster of ages between 7.9 and 9.3 ka suggests that these moraines are associated with the Hailong advance recognized by Owen et al. (2003) in valleys ~20 km to the northwest of our site. This age range, in combination with displacements between 45 and 59 m, suggests that lateral slip rates at this site are in the range of 4.8–7.4 m/k.y. We regard this as a minimum bound on the slip rate across the Anyemaqen Shan, given the fact that we do not account for the minor component of dip slip observed at this site and the possibility of additional structures along the southwestern margin of the massif.

East Kending Na Site

East of the Anyemaqen massif site, the Kunlun fault follows a series of broad valleys for ~100 km along a strike of ~110°. East of the town of Dawu (Figs. 1 and 4A), the fault forms a linear trace along the foot of an ~4000-m-high range. We explored a site near ~100.6°E, at the small

TABLE 1. SAMPLE ^{10}Be EXPOSURE AGE ANALYSIS RESULTS

Sample site	Elevation (m)	Context	^{10}Be (atoms/g qtz)	Error†	Production rate (atoms ^{10}Be per g qtz/yr)§	Exposure age (yr B.P.)	Error
Qi Er Er							
NH-KCOS-04-C1	3459	T4	691,527	36,367	49	14,015	1557
NH-KCOS-04-CHR3	3460	T4b	867,744	25,714	49	17,533	1550
East Kending Na							
NH-KCOS-04-VD1	4255	M.C.*	892,681	33,809	76	11,814	1140
NH-KCOS-04-VD2	4270	M.C.	1,102,379	38,145	76	14,477	1350
NH-KCOS-04-VD3	4262	M.C.	1,228,596	56,779	76	16,211	1698
NH-KCOS-04-VD5	4204	M.C.	1,548,691	58,196	74	21,027	2023
Anyemaqen Massif							
NH-KCOS-05-MM1	4474	M.C.	227,347	27,226	91	2490	299
NH-KCOS-05-MM2	4507	M.C.	294,876	13,576	93	3180	146
NH-KCOS-05-MM3	4500	M.C.	452,416	60,363	92	4910	656
NH-KCOS-05-MM5	4430	M.C.	735,490	29,605	89	8264	333
NHMM06-2	4491	M.C.	806,120	21,771	92	8762	237
NHMM06-6	4458	M.C.	794,948	19,281	89	8932	217
NHMM06-7	4467	M.C.	811,618	26,026	90	9018	289
NHMM06-9	4410	M.C.	1,313,565	130,857	86	15,200	1522

Note: Samples from East Kending Na were processed and analyzed at the Purdue Rare Isotopes Measurement (PRIME) laboratory. All other samples were processed at the (former) Dartmouth cosmogenic laboratory and analyzed at the PRIME laboratory.

*Moraine crest.

†Reported errors reflect analytical uncertainties only.

§^{10}Be production rates were calculated as the low-latitude production rate of Lal (1991) corrected for latitude, altitude, and topographic shielding following Stone (2000).

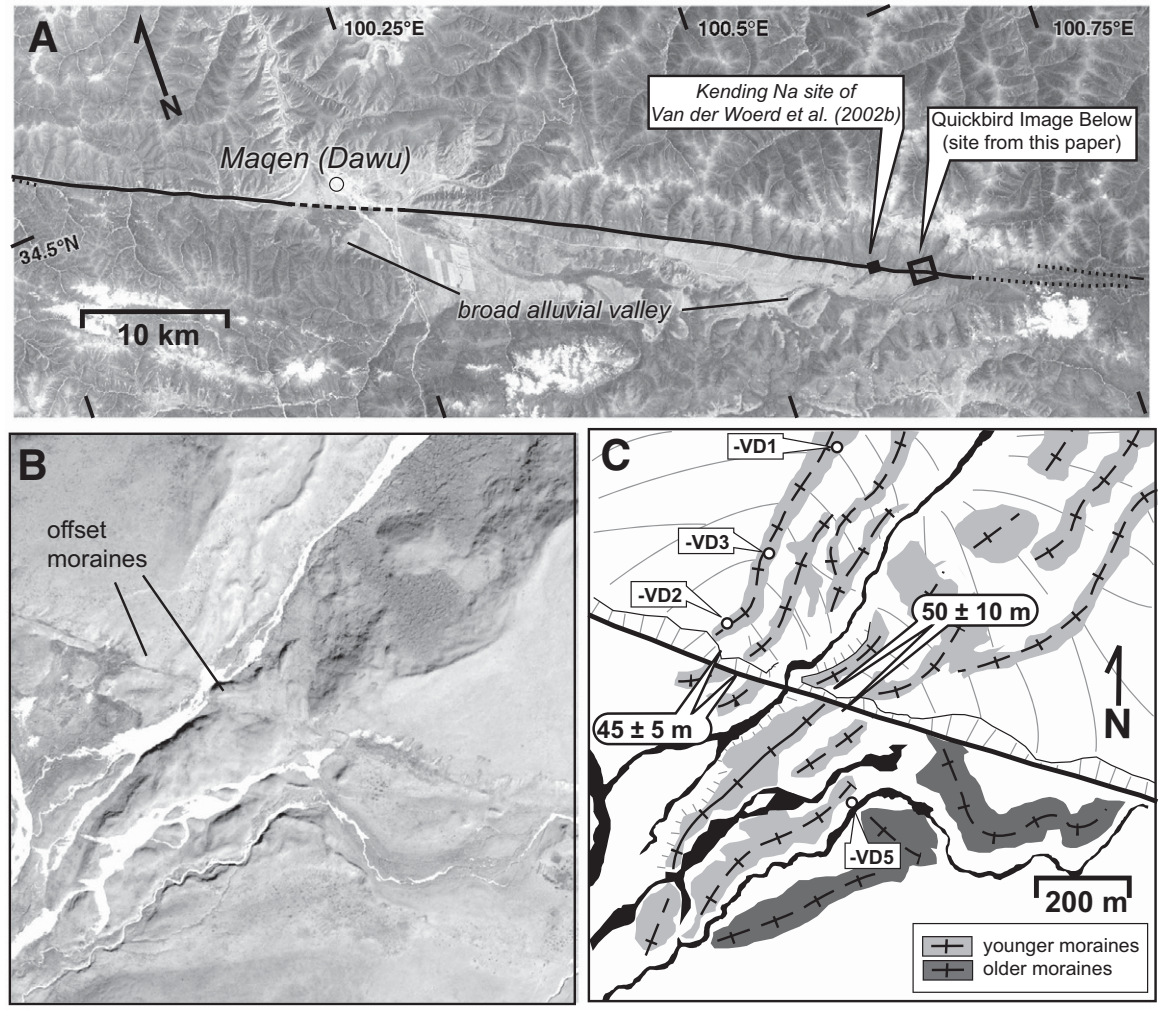

Figure 4. (A) Landsat image of the portion of the Kunlun fault hosting the East Kending Na site. (B–C) Quickbird satellite image and interpreted map of the offset moraines at the East Kending Na site; measured offset magnitudes are shown. Two ages of moraines are delineated, and sample locations are shown on the interpreted map.

watershed of Kending Na. We refer to this site as East Kending Na, to distinguish it from the site ~2 km west discussed by Van der Woerd et al. (2002b). East Kending Na is located at high elevation (~4270 m), and glaciers flowing from the northern ranges deposited moraine complexes across the active trace of the Kunlun fault. Modern glaciers are not present in the range.

The character and distribution of the deposits along the mouth of East Kending Na suggest the presence of two moraine groups of different age. Moraine ridges on both sides of the host channel were identified on remotely sensed images and surveyed with differential GPS (Figs. 4B and 4C). The first group of moraines exhibits relatively subdued topography and surfaces that are largely devoid of boulders and is only preserved southeast of the valley mouth. We did not find any correlative deposits west of the present-day drainage. Although it appears that these moraines may have been displaced to the east by slip along the fault, the absence of correlative deposits north of the fault precludes their use as a piercing point. A younger group of moraines, however, is preserved in a more proximal position to the valley mouth, and these deposits appear to correlate to moraines preserved along the inner valley walls. These moraines are characterized by relatively sharp crests and more abundant boulders exposed at the surface.

Within the younger, sharp-crested moraines, a pair of parallel ridges, spaced ~30 m apart on the west side of the active drainage are identified on both sides of the fault. Due to the similarity of this spacing and moraine morphology, as well as the lack of other moraine ridges on this side of the host channel, reconstruction of these features across the fault suggests ~45 ± 5 m of left-lateral offset since deposition. Similarly, two ridges on the east side of the host channel also appear to correlate across the fault trace. These features suggest a similar magnitude of left-lateral displacement along the fault of ~50 ± 10 m. Reported error ranges in offset magnitudes reflect uncertainties associated with projecting the subtle moraine topography across the fault zone at this site. Here, we take the same approach to quantifying uncertainty in moraine ridge crest position as was described for the Anyemaqen Massif site. Although these correlations are tentative, the similar magnitudes of displacement suggested by four independent markers suggest that slip at this site since emplacement of the moraines is 45–50 m. We note that lateral erosion by the modern fluvial channel makes it extremely unlikely that ridges east of the channel have been

displaced across the watershed mouth (supplemental Fig. DR4 [see footnote 1]). This inference constrains displacements to less than ~60 m, and we therefore reason that fault displacement at this site is 50 ± 10 m since emplacement of the moraine complex.

Moraine Ages and Slip Rates

Similar to the Anyemaqen site, we were unable to find a large number of boulders of sufficient size to be suitable for sampling (>1 m). Consequently, we determined ^{10}Be exposure ages from only four boulders at this site. These were all taken from granite boulders exposed on the younger moraines, three of which were from the north side of the fault. On the north side of the fault, all samples were taken from boulders, 2+ m in size, located on or near the crest of the lateral moraine ridge on the west side of the source valley (Fig. 4C). Two of these samples yielded overlapping ranges of exposure ages of 14.5 ± 1.4 ka (Table 1, sample -VD2) and 16.2 ± 1.7 ka (-VD3), whereas the third sample (-VD1) returned a younger exposure age of 11.8 ± 1.1 ka. The sample from the south side of the fault was extracted from an ~1-m-sized boulder located on the crest of a small moraine at the eastern edge of the younger moraines (-VD5). This sample returned a somewhat older exposure age of 21 ± 2.0 ka. As at the Anyemaqen site, the sparse data set and relatively large degree of scatter preclude a precise age determination for these moraines. However, the data clearly indicate that these moraines were deposited pre-Holocene, and we consider that the most likely age range is between ca. 12 and 20 ka, within the range of the Qiemuqu glacial (Owen et al., 2003).

Taking into account both uncertainties associated with the reconstruction of moraines and exposure ages, slip rates of 1.7–5.6 m/k.y. are permissible at the East Kending Na site. Despite the fairly wide range of allowable rates, even the maximum slip rate is considerably slower than the 12.5 ± 2.5 m/k.y. slip rate interpreted at the adjacent Kending Na site by Van der Woerd et al. (2002b). Given the similarity in interpreted ages of the moraines used to constrain fault rates at the two Kending Na sites, this striking difference in slip rates between locations is difficult to reconcile. We note, however, that the ca. 12 ka age constraint cited by Van der Woerd et al. (2002b) does not reflect actual offset moraine ages, but rather the age of a terrace generated sometime after moraine deposition. As a result, there exists the possibility that the offset moraines at the Kending Na site of Van der Woerd et al. (2002b) are significantly older than 12 ka and thus slip rates recorded by these features are actually somewhat slower.

Ola Xu Ma Site

Our third new slip-rate site is near the town of Ola Xu Ma, ~40 km east of the Kending Na site (Fig. 1B). Thirty km west of the Ola Xu Ma site, the Kunlun fault splays into at least two parallel strands as it passes through a high topographic divide. East of the divide, the fault zone follows a single nearly E-W–striking strand that follows the linear range front on the south side of a strike-parallel valley for ~15 km. Approximately 3 km west of the Ola Xu Ma site, the range front beds to the south, away from the fault zone (Fig. 5A). The Ola Xu Ma site is located ~1 km north of the range front at ~101°E, along a large tributary to the Yellow River that flows northward, orthogonally across the trace of the Kunlun fault.

At this location, a flight of four extensive fill terraces (T1–T4) and two less extensive inset terraces (T2b and T3b) is preserved on the west side of the tributary (Fig. 5B and 5C). The T4 surface is the most spatially extensive and coalesces with the uppermost surfaces of other alluvial fans emerging from the bedrock highlands to the south. These terraces and associated risers are left-laterally offset across the trace of the fault. The T2, T3, and T4 terrace treads are preserved at 5.5, 7, and 9 m above the modern flood plain, respectively (supplemental Figs. DR5 and DR6 [see footnote 1]). Lacking a wealth of radiometric age control at this site, the geologic relationships described here are critical to our interpretation of local terrace surface abandonment chronology. The T1 through T3b surfaces are capped by ~0.5 m of loess that is underlain by a 0.2–0.5-m-thick mixed sand and gravel layer. Clasts within this layer do not possess pedogenic carbonate rinds. A 0.1-m-thick layer of centimeter-sized gravel at the base of the mixed layer is observed to have a distinctive rusty color within a soil pit excavated into the T2 surface (sample site WOX-1, Fig. 5C; supplemental Fig. DR7 [see footnote 1]). Within the soil pit, this "rusty" layer is in turn underlain by coarse gravel with rare intercalated sand lenses that extends to the base of the pit. The undersides of clasts within this gravel possess well-developed pedogenic carbonate accumulations. In addition to the T2 surface, this coarse gravel is also observed in natural exposures under the T1, T3, and T3b surfaces below the loess-gravel contact.

We used the horizontal offset of terrace risers and the abandonment age of an associated terrace tread to place bounds on millennial slip rates at this site. Riser offsets were determined based on the positions of surveyed slope breaks at riser toes. Because risers follow a complex path in map view and are disrupted within the fault zone, we estimated conservative uncertainties in measured offsets associated with the projection of risers up to the fault plane. The T2/T3 and T3/T4 risers record left-lateral offsets of 30 ± 5 m and 48 ± 5 m, respectively. Since the T2/T3 riser must be older than the T1/T2 riser, the observed difference in offset magnitudes between the two riser faces is internally consistent. There is little difference in the elevations of terrace surfaces across the fault zone, indicating that the dip-slip component of fault displacement is small at this site. We note, however, that the broader fault zone is structurally complex at this location. The main trace of the fault divides into a number of splays immediately east of this site, and the linear range fronts to the south and north may host unidentified fault zones with significant dip-slip components of motion. As a result, this site is likely to record only part of the total displacement across the fault zone, and we interpret the slip rate here as a minimum bound on the total displacement rate budget at this location.

Age of the T4 Terrace and Slip Rates

Two samples of in situ, depositional organic material extracted from beneath the T2 and T3b terrace surfaces were subjected to ^{14}C age analysis (supplemental Fig. DR6 [see footnote 1]; Table 2). A snail shell extracted from a sand lens within the coarse gravel in a soil pit ~1 m below the loess-gravel contact in the T2 surface yielded an age of 15,196 ± 741 cal yr B.P. A second snail shell extracted from the base of the mixed sand and gravel layer within the T3b deposit yielded an age of 14,853 ± 656 cal yr B.P. Terrace ages at this site are difficult to interpret in light of the overlapping ages of these two samples. If these samples recorded terrace abandonment ages, the sample extracted from the T2 surface would be expected to be younger than the T3b sample. Additionally, if the ca. 15 ka sample age represents an abandonment age of the T2 surface at this site, then age-equivalent examples of the multiple younger terrace surfaces observed at sites to the east (Deng Qin and Ken Mu Da) are not preserved at this location. Alternatively, since total riser relief is small and gravels at depth are outwardly similar under all terraces at this site, we interpret the T1–T3b surfaces here as cut terraces inset into a single ca. 15 ka gravel fill. Under this interpretation, abandonment of the T4 surface would have initiated sometime between ca. 15 and ca. 14 ka, consistent with the abandonment age of the extensive T4 surface at Deng Qin and Ken Mu Da.

Although we possess little direct age control at this site, we proceed with the interpretation that terrace abandonment events were climatically moderated and roughly synchronous with dated terrace abandonment events at Deng Qin and Ken Mu Da. Abandonment of the T4 surface at 14–15 ka and the 42 ± 5 m offset of the T3/T4 riser defines a range of

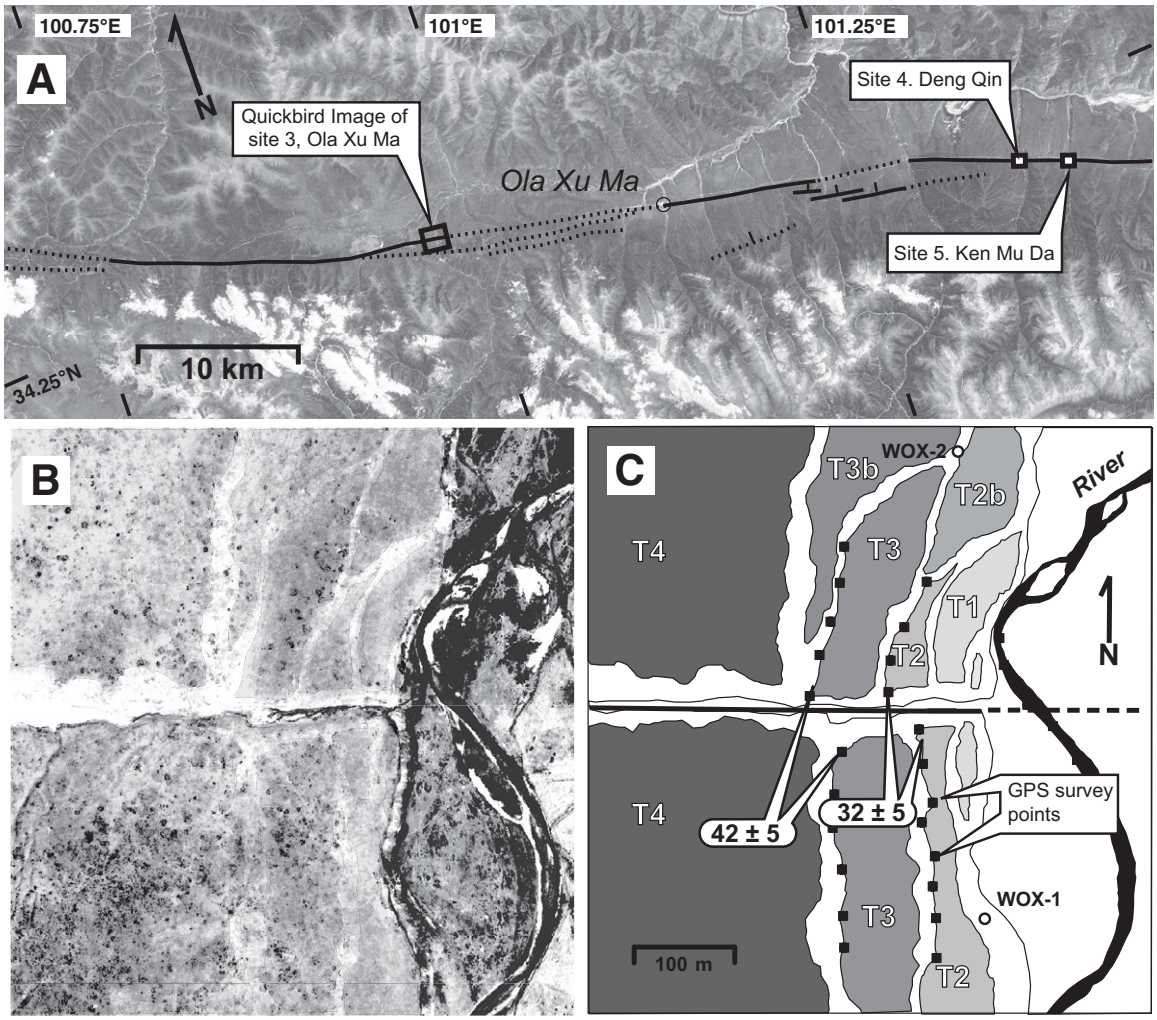

Figure 5. (A) Landsat image of the portion of the Kunlun fault hosting the Ola Xu Ma site. The town of Ola Xu Ma, the Deng Qin site, and the Ken Mu Da site are also identified. (B–C) Quickbird satellite image and interpreted map of offset terraces and risers at the Ola Xu Ma site. Global Positioning System (GPS) survey points along riser toes are delineated, offsets of these risers are labeled, and sample locations are identified.

minimum allowable slip rates at this site of 2.5–3.4 m/k.y. (Fig. 6). Additionally, if the abandonment ages of the T3 and T2 surfaces at this site are similar to those at Ken Mu Da (9–10.6 and 6–7 ka, respectively), then the 32 ± 5 m offset of the T2/T3 riser records a slip rate range of 2.6–6.2 m/k.y. The minimum slip rate of this range is corroborated by the minimum rate recorded by the T3/T4 riser dated by the ^{14}C samples at this site, suggesting that our interpretations of terrace ages and fault slip rates are valid. We therefore interpret a likely range of rates at this site of 2.5–6.2 m/k.y.

Additional Constraint at the Ken Mu Da and Deng Qin Sites

Between the Ola Xu Ma site, at ~101° E, and the Roergai Basin, at ~102° E, the trace of the fault shares a broad, strike-parallel valley with the Yellow River (Fig. 5A). Immediately east of the Ola Xu Ma site, the Kunlun fault splays into multiple strands and is distributed throughout a complex of low-relief bedrock hills. A distinct trace of the fault is absent between these bedrock hills and the town of Ola Xu Ma, which lies ~5 km east of the hills. Near the town of Ola Xu Ma, a distinct strike-slip trace of the Kunlun fault is observable in remotely sensed images that strikes ~100°. This trace of the fault extends eastward for ~30 km across a series of bajadas that head into bedrock highlands to the south. Running roughly parallel with this trace of the fault, a series of kilometer-length, right-stepping normal fault scarps trends along the base of the highlands to the south. Uplifted fluvial terraces in the footwalls of these faults (within the bedrock range) display several meters of vertical displacement. Several gullies and rills that are obliquely offset by these faults record primarily vertical displacement and little accompanying horizontal component. At ~101.3°E, the normal fault scarps abut against bedrock hills that extend northward into the Yellow River valley. From this location eastward to the slip-rate sites at Deng Qin and Ken Mu Da, at ~101.4°E, the Kunlun fault assumes a single distinct trace at the northern foot of these hills.

Two radiocarbon samples exist in addition to those reported in Kirby et al. (2007) and Harkins and Kirby (2008) that further support the interpreted age of the T4 terrace at Deng Qin and Ken Mu Da (Table 2). At Deng Qin, snail shells extracted from the gravel capping the T4 surface (sample AA60726) returned an age of 16,484 ± 471 cal yr B.P. Since the associated gravel must have been deposited just prior to abandonment of the T4 surface, this sample age further constrains a 14–15 ka timing of

TABLE 2. SAMPLE RADIOCARBON AGE ANALYSIS RESULTS

Sample site	Lab number*	Terrace surface	Stratigraphic context	Type†	$\delta^{13}C$	^{14}C age		Calendar age§	
						(yr B.P.)	Error	(yr B.P.)	Error
Tazang									
TZ1	AA60729	–	Base of soil	C	–26.82	8133	48	9173	111
TZ1	AA60730	–	Soil	P	–29.02	4168	50	4752	137
Ouarr Goth Qu									
OGC1	AA45225	T2	T2 gravel	S	–7.7	10527	77	12175	75
OGC1	AA60722	T2	T2 gravel	C	–23.1	8661	49	9668	71
OGC1	AA62942	T2	T2 gravel	C	–25.47	9600	1500	9171	1862
OGC1	AA62943	T2	T2 gravel	S	–5.62	11808	66	11831	280
OGC2	AA65886	T1	T1 gravel/loess	S	–9	5827	69	6673	173
OGC2	AA65887	T1	T1 gravel/loess	C	–24.8	6345	53	7311	159
OGC2	AA65888	T1	T1 gravel	S	–8.2	6343	49	7310	157
Qi Er Er									
QHR3	AA65892	T2	T2 gravel	C	–23.4	8806	53	9956	244
Ken Mu Da									
KMD3	AA72498	T1	Soil atop T1	S	–6.5	3060	120	3270	330
KMD3	AA45224	T1	Soil atop T1	C	–22.7	4497	51	5142	167
KMD2	AA45223	T3	T3 gravel	P	–16.3	10660	120	12565	435
KMD4	AA74003	T4	T4 loess cap	S	–6.2	11930	59	14002	317
KMD1	AA56951	T4	T4 gravel	S	–7.05	13024	75	15382	742
Deng Qin									
DQ4	AA45219	T2	Soil atop T2	S	–25.1	3166	38	3370	100
DQ3	AA72500	T4	T4 gravel/loess	S	–5.6	12325	87	14515	581
DQ2	AA60720	T4	T4 gravel	S	–6.31	13788	67	15138	697
DQ2	AA60726	T4	T4 gravel/loess	S	–6.365	13682	66	16484	471
DQ1	AA56950	T5	T5 loess cap	S	–5.74	28470	300	N.D.	N.D.
Ola Xhu Ma									
OX1	AA65883	T2	T2 gravel	S	–6.3	12819	69	15196	741
OX2	AA65884	T2	T2 gravel	S	–6.4	12364	86	14852	695
North Anyemaqen									
NA1	AA74009	–	Gravel	C	–27.1	R.D.#	–	–	–
NA1	AA74010	–	Gravel	S	–1.9	28460	300	N.D.	N.D.

*All samples were analyzed at the University of Arizona Accelerator Mass Spectroscopy Laboratory.
†Refers to the organic material dated: C—charcoal, P—peat, S—gastropod shell.
§Sample calibration was conducted using Calib 4.3 (Stuiver et al., 1998). N.D.—calendar ages not determined due to advanced sample ages; yr B.P.—years before present.
#Radiocarbon dead.

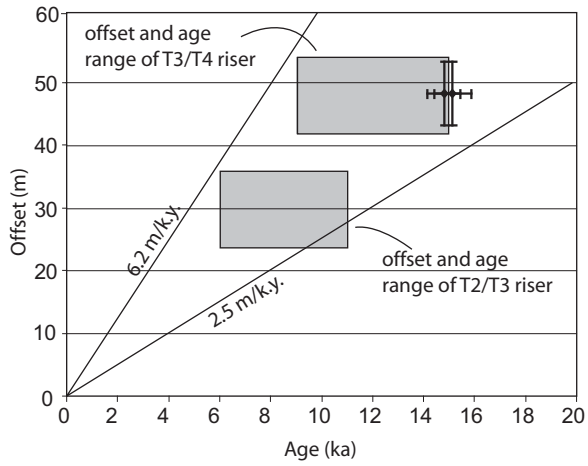

Figure 6. Sample ages plotted according to the fault offset recorded by the T3/T4 riser at the Ola Xu Ma site. These samples are interpreted to provide a maximum age of the T3/T4 riser face. Gray boxes portray the offsets recorded by the T3/T4 and T2/T3 risers if the T2, T3, and T4 surfaces share similar formation ages as the T2–T4 surfaces at Ken Mu Da. Age/offset trends for the minimum and maximum slip-rate bounds at this site are shown.

abandonment for this surface. At Ken Mu Da, a snail shell extracted from the base of the loess capping the T4 surface (sample AA74003) yielded an age of 14,002 ± 317 cal yr B.P. Since this material must have been deposited shortly after abandonment of the T4 surface, this age confirms the younger limit at 14 ka for abandonment of the T4 terrace.

Qi Er Er Site

The Kunlun fault is expressed as a single trace between the Ken Mu Da site and the next slip-rate site to the east, along the Qi Er Er River (Fig. 2A). Along the 15 km of strike length that separates the two sites, the fault strikes ~110° and cuts through a series of bajadas that head into bedrock highlands to the south. To the east, the trace of the fault is progressively further removed from the range front of these highlands. The north-flowing Qi Er Er River orthogonally crosses the active trace of the Kunlun fault at ~101.57°E, where the trace of the fault is separated from the range front to the south by ~2 km.

At Qi Er Er, flights of terraces preserve left-lateral offset risers on both sides of the host channel, although several subsidiary terrace levels are locally preserved on the east side of the channel immediately upstream of the fault intersection (Fig. 7). Slope breaks at riser toes were surveyed on both sides of the channel, and a high-resolution GPS survey was conducted on the offset risers on the east side of the channel (Fig. 7B). Five terrace levels identified based on elevation and tread surface morphology were surveyed on the east side of the channel at this site, T1, T2, T2b, T3, and T4. Immediately north of the fault, these terrace treads are ~2, 14, 16, 19, and 22 m above the modern floodplain, respectively (supplemental Fig. DR8 [see footnote 1]). Immediately south of the fault, these treads are ~2, 13, 15, 16.5, and 18 m above the floodplain, respectively. A north-side-up fault scarp is developed in the T2, T3, and T4 terraces, with vertical separations across the fault zone of 1, 2.5, and 4 m between the treads, respectively. No scarp is developed in the T1 surface. As a result, we take the differences in tread elevations to be the result of a systematic vertical, north-side-up component of fault motion since the time of T5 abandonment. North-side-up scarps are also developed in the T2b and T4 treads on the west side of the host channel. Tread elevations and scarp heights on the west side of the channel are approximately equivalent to those on the east.

Most of the terrace treads at this site exhibit subdued bar and swale topography that is relict from fluvial deposition and burial by ~1–2 m of loess. The lowest surface, T1, displays pronounced bar and swale topography, with only thin loess accumulations confined to swales. Clasts within terrace and modern channel gravels are almost exclusively granitic in composition, and originated from a Mesozoic intrusive complex in the Qi Er Er headwaters. Granite clasts observed in natural exposures and soil pits appear unweathered, even on the highest terraces, suggesting a relatively young age. Terrace and modern gravels are composed of mostly cobble-sized to ~1-m-scale boulder-sized clasts with occasional 3+ m boulders. The largest of these boulders protrude from the loess accumulations on terrace treads. Notably, we did not observe "older" gravel deposits that make up terrace straths at sites to the west. However, thick accumulations of the "older" gravel deposits are observed in extensive exposures farther downstream, at the confluence of the Qi Er Er and Yellow Rivers.

On the east side of the channel, the T3/T4 riser and a boulder levee preserved on the T3 tread are left-laterally offset by 39 ± 5 m and 35 ± 5 m, respectively. The riser above the T2 surface, which is horizontally offset by 22 ± 5 m (Fig. 8), lies at the base of the T3 tread north of the fault trace, and at the base of the T2b tread south of the fault trace. Since this riser must have been refreshed during or after the abandonment of the T2b surface, the maximum age of this riser must therefore be equivalent to the abandonment age of the T2b surface, and the minimum age should be the abandonment of the T2 tread itself. No apparent offset is observed in the

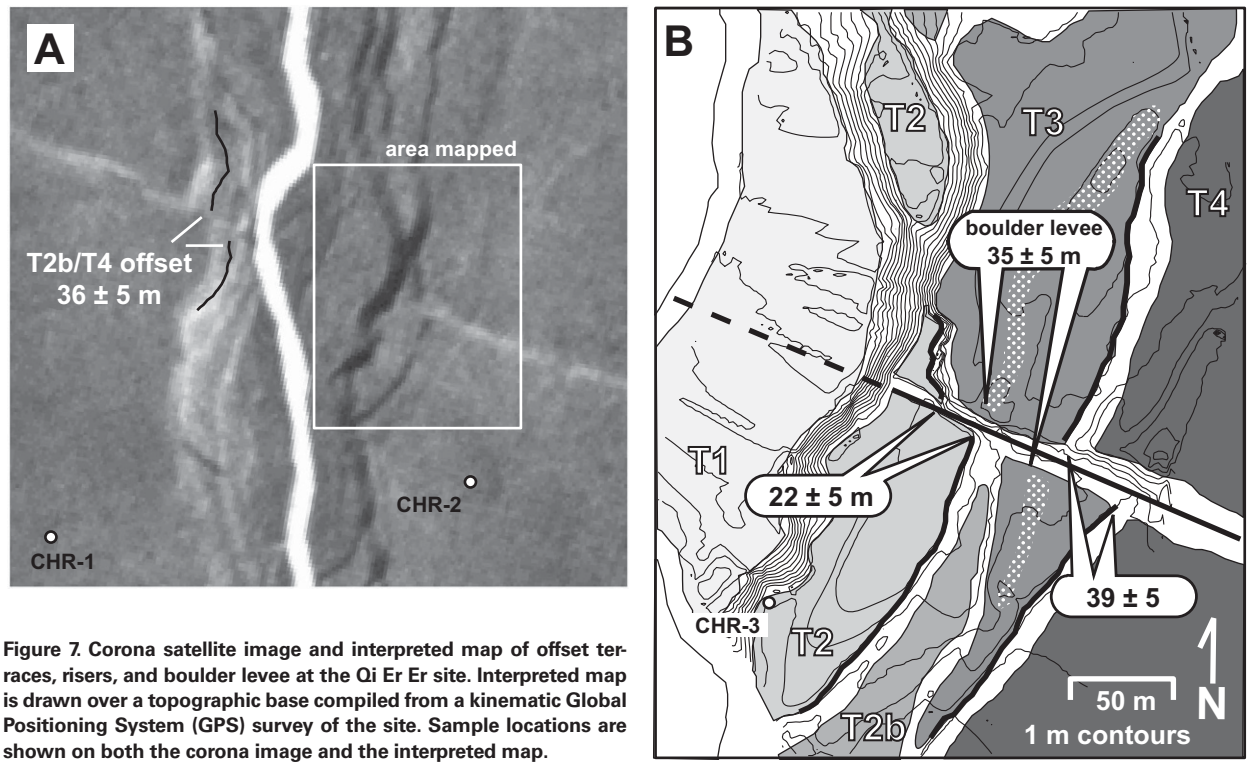

Figure 7. Corona satellite image and interpreted map of offset terraces, risers, and boulder levee at the Qi Er Er site. Interpreted map is drawn over a topographic base compiled from a kinematic Global Positioning System (GPS) survey of the site. Sample locations are shown on both the corona image and the interpreted map.

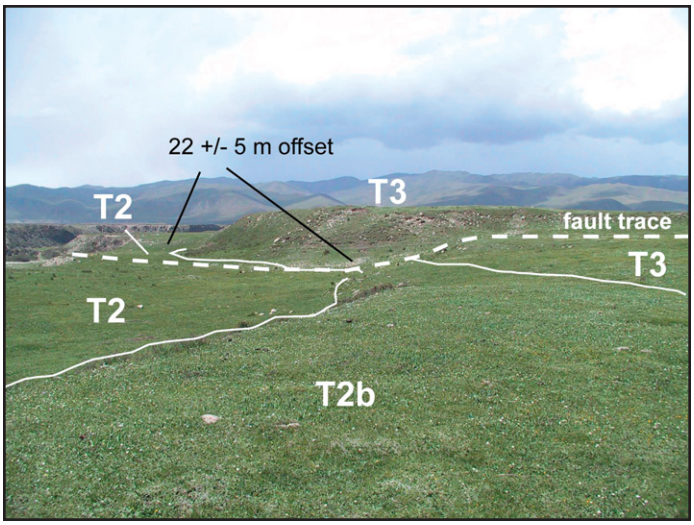

Figure 8. Interpreted field photograph of the 22 ± 5 m offset of the T2/T2b-T3 riser at the Qi Er Er site. View is to the NW across the trace of the fault zone.

T1/T2 riser, and we take this as an indication of relatively recent lateral erosion during fluvial occupation of the T1 tread.

On the west side of the valley, ongoing lateral erosion by the modern channel has obliterated most of the terrace risers (Fig. 7), leaving only the highest unmodified. We measured the lateral displacement of the T2b/T4 riser using a handheld laser rangefinder and determined a displacement of 36 ± 5 m. The similarity of this measurement to displacements observed east of the valley gives confidence that this is a reliable estimate of fault displacement subsequent to development of the T2b terrace surface.

Terrace Ages and Slip Rates

Constraints on terrace abandonment age at this site are provided by both ^{14}C and CRN analysis of terrace gravel material. The ^{14}C analysis of a single piece of charcoal extracted from within fluvial gravels ~20 cm below the gravel-loess contact on the T2 surface yielded an age of 9956 ± 244 cal yr B.P. (Table 2). Because this sample was extracted from very near the top of the gravel capping the T2 surface, we take this sample age to closely approximate the abandonment age of the T2 surface. From a regional standpoint, this date suggests that the terrace is broadly equivalent to early Holocene terraces at Ken Mu Da (locally, T3) and at Ouarr Goth Qu (locally, T2).

In addition, two boulders exposed on terrace treads were sampled for CRN exposure age analysis (Table 1). Sampling strategy and processing of these samples were the same as the moraine boulder samples described at the Anyemaqen and East Kending Na sites. Both sampled boulders were granitic in composition and protruded more than 0.5 m above the terrace tread (supplemental Fig. DR9 [see footnote 1]). The first boulder (CHR-1), located on the intact T4 surface on the west side of the channel ~400 m south of the fault trace, yielded an exposure age of 14.0 ± 1.6 ka. The second sampled boulder (CHR-2), located on a small inset surface in the T4 tread on the east side of the channel ~200 m from the fault trace, yielded an age of 17.5 ± 1.6 ka. Because the base of the CHR-2 boulder is broad and the top extends well above the T4 surface, it is unlikely that the sampled portion of this boulder was ever buried after deposition of the T4 surface. Thus, although we only have two CRN ages here, they are consistent with occupation of the T4 surface sometime between ca. 12.4 and 19.1 ka.

Although two exposure ages are, in isolation, not sufficient to reliably date abandonment of the T4 tread, three lines of argument suggest that these ages provide a reasonable approximation. First, the morphologic character and landscape position of the T4 terrace as an extensive, broad surface suggest correlation with the highest terraces at Deng Qin and Ken Mu Da (T4) and at Ouarr Goth Qu (T3). Second, the CRN ages overlap with these well-dated surfaces (T4 at Deng Qin and Ken Mu Da ca. 15 ka, and T2 at Ola Xu Ma ca. 15 ka). Thus, we consider it likely that these surfaces were abandoned nearly synchronously, probably in response to deglaciation of their headwaters during the latest Pleistocene. Third, the charcoal from the inset T2 surface places a minimum constraint on the abandonment of T4 of ca. 10 ka. Thus, the CRN ages are not unreasonably old, as might be the case if inheritance were a significant component of ^{10}Be concentrations.

Given that the range of displaced markers at this site (T3/T4 riser, 39 ± 5 m; T2b/T4 riser, 36 ± 5 m; and T3 boulder levee, 35 ± 5 m) suggests 30–45 m of displacement, we can be reasonably confident of the minimum slip rate. If the oldest CRN age (ca. 19 ka) is taken as a measure of T4 abandonment, then the slip rate must be at least ~1.6–2.4 m/k.y. (Fig. 9). If, however, the T4 terrace was abandoned closer to ca. 15 ka, as suggested by the regional correlation with well-dated sites, then the corresponding minimum slip rate is a bit higher, between 2.0 and 3.0 m/k.y.

Estimating the maximum allowable slip rate at this site is a bit more uncertain, and relies heavily on the radiocarbon age from T2. If the 22 ± 5 m of displacement of the T2/T2b riser accumulated after abandonment of the T2 tread, this suggests that maximum allowable slip rates over the past 10 k.y. have been between 1.7 and 2.7 m/k.y., similar to the minimum rates discussed previously. However, the T2/T3 riser north of the fault is strongly curved, suggesting that it may have been eroded somewhat during development of the T2 tread (Fig. 7). If this was the case, the true offset could be somewhat greater, implying correspondingly greater slip rates. Displacements of markers associated with T3 and T4, however, allow us to estimate an absolute maximum slip rate.

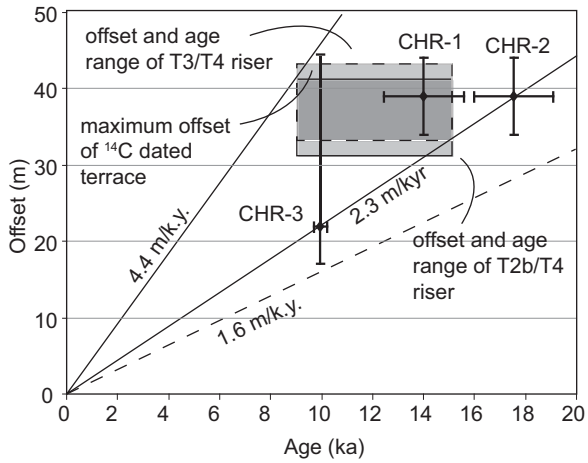

Figure 9. Sample ages plotted according to the fault offset recorded by the T3/T4 and T2/T2b-T3 risers at the Qi Er Er site. The two older samples are interpreted to provide a maximum age of the T3/T4 riser face. The younger sample is interpreted to provide a minimum age for the T2/T3 riser face. Gray boxes portray the offsets recorded by the T3/T4 and T2b/T4 risers if the T2, T3, and T4 surfaces share similar formation ages as the T2–T4 surfaces at Ken Mu Da and Ouarr Goth Qu. Age/offset trends for the minimum and maximum slip-rate bounds at this site are shown.

It is clear that the entirety of 30–45 m displacement observed from the T3/T4 features must have accumulated subsequent to abandonment of T2. Thus, slip rates over the past 10 k.y. could not have been greater than 3.0–4.5 m/k.y. at this site. Our preferred correlations (T4 with the regional ~14–15 ka terrace abandonment event) lead us to argue that the most likely slip rate at this site is 2.3–4.4 m/k.y.

SUMMARY OF MILLENNIAL SLIP RATES

In this work, we discuss all slip rates as the range of allowable rates rather than the more commonly reported mean value with an uncertainty range. Lacking additional geologic constraint, we regard all rates within reported ranges to be equally likely. Our new results are consistent with previous studies of Kirby et al. (2007) and show that millennial slip rates along the eastern Kunlun fault generally decrease eastward, decreasing to ~1 mm/yr near ~102°E (Fig. 10). Thus, the primary implication of our results is that the slip rate along the Kunlun fault during the latest Pleistocene and Holocene varies strongly over the eastern 200–300 km of the fault system. It appears that most of the modern slip along the Kunlun fault system terminates near the town of Maqu, well west of the eastern margin of the Tibetan Plateau.

The median values of the slip-rate ranges at the East Kending Na and Ola Xu Ma sites are low when compared to the slip rates at Deng Qin and Ken Mu Da. We emphasize that this may in part be due to the large range of allowable ages of offset features at these sites, rather than actual likelihood of slower rates. Geometric complexity and the presence of multiple fault strands near Ola Xu Ma, however, may also explain why slip rates at this site are low relative to sites farther east (Fig. 10); additional displacement may be present on additional fault strands within the Kunlun fault zone. Similarly, East Kending Na is located just west of an area where the trace of the Kunlun fault becomes obscure, implying that slip may be distributed over a wider zone of faults rather than along a single fault plane. Although second order to the overall trend of decreasing slip rates to the east, these effects reflect the kinematic complexity of the eastern Kunlun fault and caution against characterizing fault-zone displacement rates based on a single location.

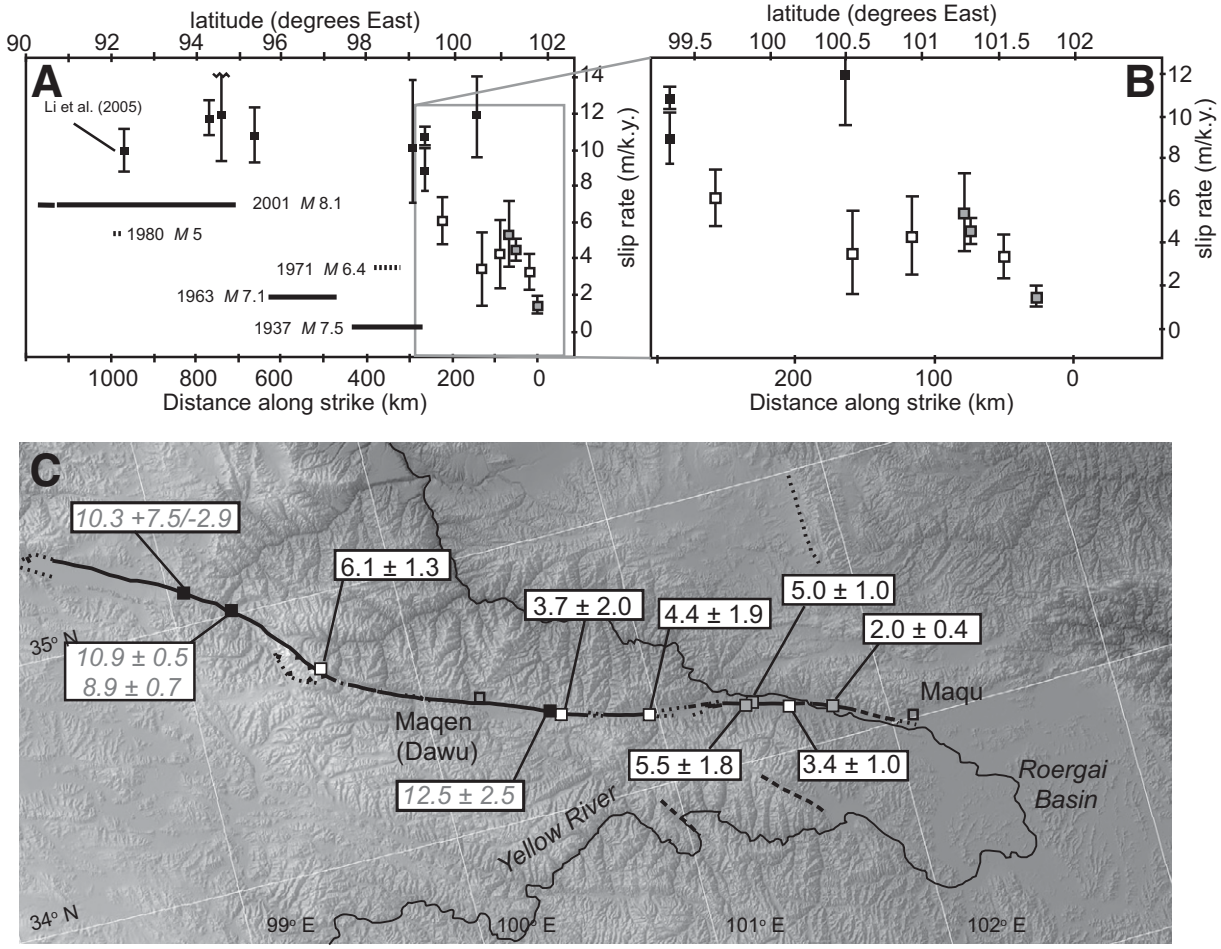

Figure 10. Plots of millennial slip rates versus distance along the Kunlun fault. Rate estimates in panels A, B, and C are symbol-keyed to their sources; black boxes are rates reported in Van der Woerd et al. (2002b) and Li et al. (2005), gray boxes are from Kirby et al. (2007) and Harkins and Kirby (2008), and white boxes are from this study. (A) Slip-rate estimates from the entire fault extent. The approximate rupture extents and dates of major seismogenic events along the fault are also shown (Li et al., 2005; Lin et al., 2002; Tapponnier and Molnar, 1977; Van der Woerd et al., 2002a). (B) Slip-rate estimates determined along the eastern Kunlun fault. (C) Shaded relief map of the locations and associated slip rates at sites along the eastern Kunlun fault. Sites discusssed in this work are in black; sites presented in Van der Woerd et al. (2002b) are in gray. Rates are displayed in m/k.y.

STRUCTURES PROXIMAL TO THE EASTERN KUNLUN FAULT

Termination of a major, rapidly slipping strike-slip fault requires that displacement somehow be absorbed by deformation of the crust adjacent to the fault system. Such deformation might be expressed as distributed deformation in the crust surrounding the leading fault tip, or it could be taken up by slip on subsidiary structures adjacent to the primary fault strand. This explanation is typically considered a means by which slip along the Kunlun fault can be transferred to the edge of the Tibetan Plateau, via faults along the valley of the Bailong Jiang (river) (e.g., Van der Woerd et al., 2002b). In this section, we present observations that place constraints on the degree of Quaternary activity along these structures.

Duo Song Valley

North of the Kunlun fault, the Duo Song River valley (Fig. 11) is bounded on the north side by a linear range front that trends subparallel to the strike of the Kunlun fault. Faceted bedrock spurs suggest that the range front is bounded by a fault zone with some degree of Quaternary dip slip (supplemental Fig. DR10 [see footnote 1]). Geomorphic evidence of slip on the fault dies out at the eastern head of the valley, and it appears that the fault terminates at this pass. We were unable to observe definitive evidence of lateral slip. However, folded pre-Mesozoic strata exhibit an apparent left-lateral separation of ~10 km across the valley, although the planar contacts do not form precise piercing points. If this separation is indicative of lateral slip, it must be a relatively ancient feature; at the eastern end of the valley, the fault is overlapped by Cretaceous–early Tertiary terrestrial sediments that are continuous across the fault. Thus, we consider the Duo Song structure to be primarily a pre-Tertiary fault that may have undergone slight reactivation during recent deformation. It does not appear to transfer a significant amount of left-lateral slip from the main Kunlun fault system.

North Anyemaqen Structure

One candidate structure that appears prominently on regional maps of Tibetan faults (e.g., Yin and Harrison, 2000) occurs ~50–100 km north of the Kunlun fault, between ~99°E and ~101°E. This structure is mapped primarily along a series of linear, E-W valleys (Fig. 11). We explored the easternmost of these valleys and discovered north-facing scarps and faceted bedrock interfluves developed along the southern margin of the valley (supplemental Fig. DR11 [see footnote 1]). These landforms suggest recent activity along a range-bounding fault.

Two ^{14}C samples were extracted from a terrace surface along a channel that crosses the range front at ~100.74°E. This terrace tread makes a broad alluvial surface across the projected trend of the range front and does not display scarps or other evidence of active faulting. Similarly, soil horizons developed in this terrace surface show no evidence of disruption across the trend of the range front. This channel is one of several channels that cross the range front in the vicinity of 100.7°E, all of which have similar terrace surfaces that do not show signs of active faulting. One of the samples, consisting of charcoal extracted from fluvial gravels ~10 cm below the 2-m-thick loess cap, did not contain enough ^{14}C for age analysis (Table 2). The second sample, consisting of snail shells extracted from the base of the overlying loess cap, yielded an uncalibrated ^{14}C age of 28,460 ± 300 yr B.P. Thus, alluvial terraces in this region appear to be quite old, >25–30 ka, and constrain the most recent event on this fault to sometime in the Pleistocene. Thus, the fault appears to be a rather minor structure and does not apparently transfer a significant amount of slip away from the primary trace of the Kunlun fault.

Awoncong Fault

South of the Kunlun fault, there are two parallel valleys that trend NW-SE (~140°) (Fig. 11). The linearity of mountain fronts along the southwestern valley walls suggests that recently active faults occupy the valleys (e.g., Van der Woerd et al., 2002b, their Fig. 27). In order to determine the possibility of fault activity and associated sense of slip, we explored both valleys. The eastern valley exhibits a sharp, linear range front along the western valley wall. Numerous faceted spurs, displaced bedrock interfluves, and scarps along the range front imply Quaternary activity along a fault zone with left-lateral displacement. We informally refer to this fault as the Awoncong fault, named for a nearby town.

Where we observed truncated and displaced bedrock interfluves, they appear to consistently be displaced in a left-lateral sense (Fig. 12). However, the majority of alluvial deposits do not appear to be cut by the fault; we only observed scarps in the highest deposits. Thus, we tentatively

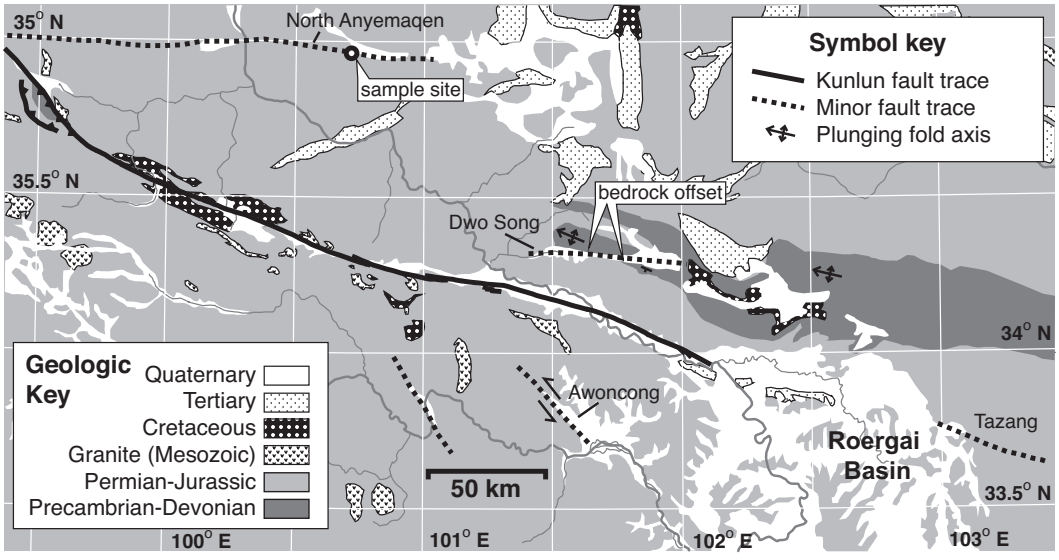

Figure 11. Simplified geologic map of the region around the easternmost Kunlun fault. Major structural features discussed in the text are labeled.

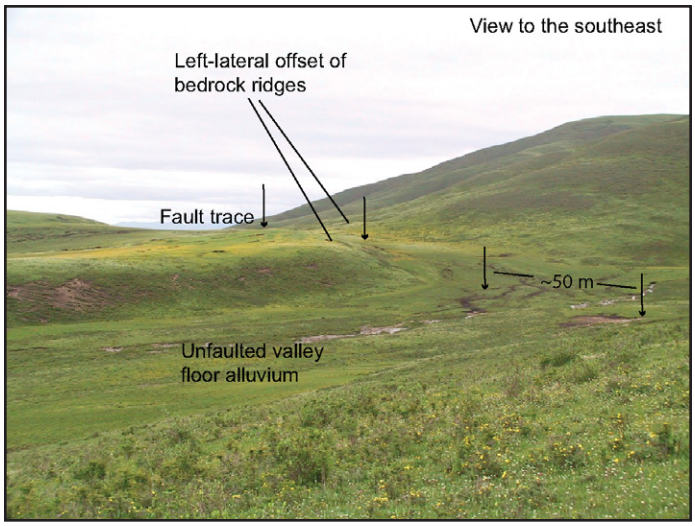

Figure 12. Field photograph from the Awoncong fault. Left-lateral and northeast-side-down bedrock offsets are apparent, although obvious offset of valley floor alluvium is lacking.

consider that this structure is also a minor fault, one that does not currently transfer a significant amount of slip from the Kunlun fault. Regardless of the slip rate, the geomorphic expression of the Awoncong fault suggests a north-side-down component of displacement. The Yellow River is entrenched in a narrow canyon in the mountains south of the fault, whereas it develops a broad floodplain with multiple threaded channels north of the fault that we interpret to reflect long-term relative subsidence of the northern fault block. Toward the northwest, the fault trace becomes indistinct in high, mountainous topography near the Kunlun fault; likewise, toward the southeast, the fault trace becomes indistinct and obscured by alluvium associated with the margin of the Roergai Basin. Thus, although the slip rate of this structure is uncertain, it probably does not act to transfer slip from the Kunlun fault to other structures. Rather, it appears to reflect deformation and perhaps NE-directed shortening surrounding the eastern tip of the Kunlun fault.

West of this structure, there is a second, northwest-trending valley that intersects the Yellow River at the small town of Muxi He. Fault-related offsets of Quaternary landforms are not observable in remotely sensed images of the Muxi He valley (both Landsat and Corona imagery). In addition, the Muxi He valley structure has a limited strike extent and does not appear to directly link up to Kunlun fault to the north. Thus, this structure does not appear likely to absorb a significant amount of lateral slip from the Kunlun fault.

DISCUSSION

Constraints on Total Displacement along the Eastern Kunlun Fault

The Kunlun fault is clearly associated with the Early Jurassic Anyemaqen-Kunlun-Muztagh suture (Dewey et al., 1988). However, the history of slip along this lithospheric boundary remains unclear largely due to the lack of any well-determined estimates of total displacement along the system during the Cenozoic. Although Fu and Awata (2007) argued for correlations among Jurassic plutons and Cretaceous basins and inferred ~120 km of displacement along the eastern Kunlun fault, the timing of this movement is highly uncertain and could have even been associated with the development of the basins themselves. Crosscutting relationships between the eastern end of the Duo Song Valley fault and an undeformed package of Cretaceous–early Tertiary sediments implies that this structure has been inactive since that time (Fig. 11). This relationship suggests at least two temporally distinct episodes of left-lateral shear: an early event that predates the early Cenozoic, and a later event that continues to the present. This history significantly complicates the interpretation of displacements inferred from displaced bedrock features, and deconvolving the Cenozoic history of slip along the Kunlun fault remains a challenge.

Seismotectonics along the Eastern Kunlun Fault

Our new results confirm earlier interpretations of along-strike variations in slip rate along the eastern segment of the Kunlun fault (e.g., Kirby et al., 2007). Slip rates over the past 10–20 k.y. decrease systematically along the Kunlun fault between ~100°E and ~102°E (Fig. 10). Because our study utilizes geomorphic markers, each of which is displaced by 20 m or more, these results represent the average rate of slip along the fault. A recent paleosesimic study along the segment of the fault near Maqu (Lin and Guo, 2008) revealed evidence for up to nine individual events during the past 10 k.y. These authors also argued from offset gullies that the lateral component of slip during the most recent event was ~2–3 m. Both of these observations are entirely compatible with slip rates of ~2 m/k.y. at the easternmost site along the Kunlun fault (Ouarr Goth Qu). More importantly, these results suggest that our slip-rate estimates are not strongly biased by seismic cycle effects. That is, low slip rates inferred at our easternmost sites still represent multiple events and are not an artifact of single- or double-event rates.

Our results thus raise the question of how such spatial variations in co-seismic strain release are accomplished. Do the higher slip rates along the Kunlun fault between Maqu and Dawu (Fig. 10) reflect more frequent earthquakes during the past 20 k.y., larger events with greater displacement, or, potentially, a greater fraction of aseismic slip? We cannot satisfactorily answer these questions at this time. However, we believe they provide strong motivation for additional paleoseismic studies along the Kunlun fault.

Kinematic and Geometric Complexity of the Eastern Kunlun Fault

Between ~100.5°E and 101.3°E, the Kunlun fault assumes a generally releasing-bend geometry relative to the trace of the fault east and west of this zone. Between Ola Xu Ma and Deng Qin, the trace of the Kunlun fault makes a prominent left step within a distinctly wide portion of its hosting valley. The southern side of this valley bears evidence of north-side-down extensional faulting in the form of normal fault scarps and a prominent linear contact between valley floor alluvium and the bedrock range front. Thus, we interpret this part of the Kunlun fault as an active pull-apart basin within a zone of transtension.

Interestingly, displacement along this portion of the Kunlun fault appears to be partitioned between predominantly strike- and dip-slip structures. Because there appears to be only a small amount of strike-slip on the normal faults active along the southern side of the valley, these normal faults thus accommodate extension associated with the pull-apart geometry. Several kilometers north of the normal-faulted range front, a discontinuous fault trace exhibits only evidence of left-lateral strike slip within the valley fill alluvium. This structure is therefore interpreted to accommodate primarily lateral slip, albeit at a slower slip rate than pure strike-slip segments of the Kunlun fault zone. Although not directly dated, the normal-faulted and uplifted fluvial terraces in the bedrock range likely

have a similar formation age to the strike-slip offset terraces at Ola Xu Ma and elsewhere. As a result, strike- and dip-slip events partitioned from the total strain budget within the releasing bend appear to be coeval, at least at timescales of thousands of years and longer.

We also note that this releasing bend in the Kunlun fault zone is developed such that the fault steps to the north of an extensive suite of granite plutons exposed at ~101.5°E (Fig. 11). Because these plutons are likely to be both mechanically stronger than the flysch country rock and more extensive in the subsurface than in outcrop, we suggest that the releasing bend is developed where shear along the Kunlun fault zone is accommodated at the edges of this granite body. This relationship implies an upper-crustal control on regional fault kinematics. Conversely, along the transpressional extent of the Kunlun fault zone, where the restraining bend has driven uplift of the Anyemaqen Massif, we do not observe evidence of this kind of dip- and strike-slip partitioning. Rather, both the contractional and horizontal shear components of fault slip appear to be accommodated by oblique motion on a single main fault trace.

Finally, we note that a geometric restoration across the releasing bend provides a crude estimate of total amount of displacement across the present trace of the Kunlun fault zone (e.g., Fu and Awata, 2007). The topography of the pull-apart restores with ~30 km of right-lateral strike-slip along an azimuth of 110°, corresponding to the trend of the adjacent pure strike-slip portions of the fault zone. Thus, the actual amount of left-lateral shear along the Kunlun fault zone associated with the formation of this pull-apart must be less than this amount. Although speculative, we note that the Kunlun fault slip rate at Deng Qin and Ken Mu Da of ~5 m/k.y. could accommodate this maximum of 30 km of displacement in ~6 m.y.

Possible Modes of Fault Termination

The strong similarity between the slip-rate gradient that our results reveal along the eastern Kunlun fault and displacement-length variations observed for non–plate boundary faults (e.g., Schlische et al., 1996) invites comparison between these data. Globally, isolated, noninteracting fault systems exhibit a systematic scaling relationship between fault length and total displacement (global average ~0.03; Schlische et al., 1996) that evolves as a competition between fault growth and accumulated displacement (cf. Cowie and Scholz, 1992; Walsh et al., 2002). Departures from this global average are easily understood as a consequence of fault interaction (e.g., Gupta and Scholz, 2000) that may drive temporal changes in fault slip rate (e.g., Gupta et al., 1998; Roberts and Michetti, 2004)

Because the evolution of crustal-scale strike-slip fault systems is difficult to characterize, there are relatively few studies that pertain directly to this class of faults. Much of the thinking about strike-slip faults derives from the work of Wesnousky (1998), who argued that the complexity of strike-slip faults (their segmentation) scales inversely with the total displacement. This model implicitly assumes that the surface expression of a strike-slip fault directly mirrors a localized shear zone at depth, and one would not expect strong spatial variations in slip rate across segment boundaries unless the boundary conditions on the shear zone also changed. Cowie et al. (2007), however, recently argued that when one looks closely at displacement-length scaling from strike-slip faults (Stirling et al., 1996), they are indistinguishable from the global average. This suggests that processes in the brittle crust may also control the growth and evolution of strike-slip faults, and thus it is possible that the displacement-rate gradient observed along the eastern Kunlun fault reflects the recent growth of the fault system.

Within this context, we consider four potential scenarios that may explain the slip-rate gradient and apparent termination of the Kunlun fault. We evaluate the likelihood of different modes of fault termination based on regional geologic observations in the context of millennial slip rates along the eastern Kunlun fault.

1. Left-Lateral Displacement along the Central Kunlun Fault Is Transferred to Adjacent Strike-Slip Faults

This is the primary mechanism by which slip along the Kunlun fault could be linked to either shortening along the margin of the plateau adjacent to the Sichuan Basin (e.g., Chen and Yang, 2004; Van der Woerd et al., 2002b) or transmitted to strike-slip faults in the western Qinling Shan (Peltzer and Saucier, 1996; Van der Woerd et al., 2002b; Zhang et al., 1998). Our observations, however, suggest that this mechanism plays a relatively minor role. First, we were unable to identify any significant structures north or south of the primary trace of the Kunlun fault that could transfer slip (and thus account for the slip-rate gradient). Faults in the northern Anyemaqen Shan either appear to predate the early Cenozoic (Duo Song fault) or to have minor displacement (North Anyemaqen and Awoncong faults). Second, the West Qinling fault system, considered a prime candidate to transfer slip toward the West Qinling Shan (Van der Woerd et al., 2002b), does not exhibit a geomorphic expression until ~103°E, nearly ~100 km east of the termination of the Kunlun fault. Moreover, recent work suggests that the slip rate along the West Qinling fault is modest, ~2–3 m/k.y. (Yuan et al., 2007). Third, faults south of the Kunlun fault appear to also die out toward the east, into the Roergai Basin. Thus, these are not obvious candidates to pass lateral slip farther east, and we are forced to consider other mechanisms that may absorb slip along the eastern Kunlun fault.

2. Displacement along the Kunlun Fault Is Absorbed by Crustal Thickening

The slip-rate gradient along the Kunlun fault could be accommodated by crustal thinning on the north side of the fault and/or thickening on the south side, assuming that the region east of the fault is acting as a fixed "backstop" relative to the fault. If crustal thickening or thinning is absorbing the entirety of ~10 m/k.y. of shear inferred along the central Kunlun fault, then we might expect relatively rapid changes in crustal thickness adjacent to the slip-rate gradient. Although the topography itself suggests the possibility of ongoing deformation (e.g., Harkins et al., 2007), there is little evidence for major shortening, such as that associated with the terminus of the Altyn Tagh or Haiyuan fault zones. Thus, although we cannot rule out the possibility of distributed rock uplift around the eastern fault termination, it seems unlikely that this accommodates all of the displacement along the Kunlun fault.

3. The Kunlun Fault Is Relatively Young and Propagating Eastward

If displacement-length scaling provides insight into fault growth, we might expect that the Kunlun fault is currently propagating eastward. Fractures in brittle solids are expected to extend their strike lengths, or outwardly propagate their tips, as some power-law function of displacement (e.g., Lawn, 1975). Although application of these simple models to a crustal-scale fault zone is certainly an oversimplification, the similarity between the observed displacement gradient and the global data set (Schlische et al., 1996) is striking. Unfortunately, the absence of definitive markers of intermediate age along this section of the Kunlun fault precludes a quantitative evaluation of the ways in which slip accumulated during fault growth. We note that the higher geometric complexity of the eastern Kunlun fault zone and the reconstruction of <30 km of strike slip across the releasing bend at Ola Xu Ma imply that the total amount of displacement here is relatively low. If the eastern segment of the Kunlun fault is relatively young, or has not experienced large magnitudes of total

strain, then the growth and outward expansion of the Tibetan Plateau is not driven by propagation of strike-slip faults (Tapponnier et al., 2001), but rather preceded development of the Kunlun fault.

4. Left-Lateral Slip along the Central Kunlun Fault Is Absorbed Via Interaction with Regional Clockwise Rotation or Distributed Shear

While geodetic data from the region east of the Kunlun fault are inconsistent with shear across E-W planes (e.g., Kirby et al., 2007), geodetic velocities reveal the presence of a distributed, dextral shear zone that trends NE-SW, i.e., nearly orthogonal to the strike of the eastern Kunlun fault (e.g., Burchfiel et al., 2008; Zhang et al., 2004). As noted previously (Kirby et al., 2007), shear in this orientation could drive a clockwise rotation of the fault that may be, in part, responsible for the displacement-rate gradient (England and Molnar, 1990). The scenario would effectively result in spatial variations in the regional strain pattern that drives fault slip, and thus could support the observed slip-rate gradient at a relatively steady-state fault strike length. There is geologic evidence that other portions of the Kunlun fault zone have experienced a significant amount of clockwise rotation as well. Yin et al. (2008) cited varying amounts of N-S–directed contraction across the Qaidam Basin as evidence of relative clockwise rotation of the Kunlun Shan, which hosts the western Kunlun fault, since the Paleogene. In light of the corroborating geodetic and geologic evidence, we consider it likely that interaction with a regional rotation or right-lateral, N-S–oriented shear zone accommodated some amount of the observed slip-rate gradient. Given the fault slip rates and the relatively small amount of total displacement in the vicinity of the Ola Xu Ma releasing bend (~5 m/k.y. and <30 km, respectively), either this scenario is a relatively young feature or slip rates have recently accelerated to their current magnitudes.

Implications for the Dynamics of Tibetan Deformation

At a basic level, the observation that slip rates decrease to near zero at the eastern end of the fault implies that slip along the fault system does not accomplish extrusion of a central Tibetan lithospheric block relative to a northern one (e.g., Kirby et al., 2007). Lithospheric block extrusion–type models have driven a great deal of thinking about Tibetan geodynamics (Avouac and Tapponnier, 1993; Tapponnier et al., 1982) and still influence interpretations of present-day velocity fields (e.g., Meade, 2007; Thatcher, 2007). Both of the latter studies predict that ~6–7 mm/yr of shear passes between Maqu and the topographic margin of the Tibetan Plateau along the Kunlun fault (Fig. 1). However, the apparent decrease in slip rates along the primary trace of the Kunlun fault and the absence of rapidly slipping structures that could transfer displacement away from the primary fault argue that shear associated with the Kunlun system dies out by ~102°E.

It is important to note that the termination of the fault system does not simply reflect differences in geodetic strain rates and geologic displacement rates. Although this argument has arisen for other intracontinental faults in Asia (e.g., Mériaux et al., 2004), geologically determined slip rates and geodetic velocities along the Kunlun fault yield similar estimates (cf. Van der Woerd et al., 2002b; Zhang et al., 2004). Strikingly, in detail, the geodetic data east of ~102°E (Shen et al., 2005) do not require any left-lateral shear along the projection of the Kunlun fault (see Fig. 6 of Kirby et al., 2007). That is, both geologic slip rates and geodetic data indicate that shear associated with the Kunlun fault decreases from west to east. As a result, these findings directly contradict block models that predict a continuous boundary between quasi-rigid blocks east of ~102°E (cf. Meade, 2007; Thatcher, 2007), and it appears that the deformation field in this region is not well described by rigid block–type displacements.

Although we cannot rule out that the Kunlun fault is still lengthening and propagating eastward, the spatial change in the geodetic velocity field along strike of the fault system suggests that the boundary conditions driving fault slip are, in part, responsible for variations in slip rate. This could reflect differences in the rheology of Tibetan crust (e.g., Hilley et al., 2009). Alternatively, this could reflect changes in the far-field stress along the fault zone, as would be the case if the slip-rate gradient were accommodated by regional rotation of the Kunlun fault zone. Regardless, the termination of such a major fault system within an active orogen is unusual and challenges some of our simple models of intracontinental deformation. Currently, we consider shortening within the surrounding crust or regional rotation of the fault zone as equally likely accommodation mechanisms for the slip-rate gradient along the eastern Kunlun fault. Potentially, both of these mechanisms could be active together, whereby the N-S–oriented dextral shear associated with the rotation is also responsible for distributed shortening in the crust surrounding the fault. Finally, we reemphasize that the detailed description of the distribution of shear along the eastern Kunlun fault provided herein could be compared to mechanical models to provide more quantitative constraint on both local lithospheric and crustal rheology and regional kinematics.

CONCLUSIONS

We used displaced Pleistocene to Holocene geomorphic features to determine slip rates at four new localities (at the Anyemaqen Massif, East Kending Na, Ola Xu Ma, and Qi Er Er sites). When considered in concert with four previously published slip rates along the eastern ~250 km of the Kunlun fault system and investigations of adjacent faults, these new slip-rates constraints allow us to draw the following conclusions:

1. Slip rates along the eastern Kunlun fault systematically decrease eastward, from >7 m/k.y. at ~99.5°E to <2 m/k.y. at ~102°E. These rates reflect averages of many earthquake cycles and appear to represent the macroscopic behavior of the Kunlun fault since at least late Pleistocene time.

2. Strain partitioning is evident within a geometrically complex, transtensional portion of the fault zone, but it is not observed within a zone of transpression. The development of a releasing bend adjacent to a large suite of granite plutons implies a degree of upper-crustal mechanical control on Kunlun fault kinematics.

3. Adjacent secondary fault zones do not appear to transfer slip away from the primary trace of the Kunlun fault system. Rather, these faults likely reflect distributed deformation in the crust surrounding the tip of the Kunlun fault.

4. The slip-rate gradient near the tip of the eastern Kunlun fault zone may indicate that the eastern segment of the fault is relatively young. Alternatively, interaction of the Kunlun fault with a zone of regional clockwise rotation and/or distributed shortening may absorb displacement along the fault.

5. Deformation in the region around the eastern Kunlun fault is poorly described by "rigid-block" style kinematic models, which predict the transfer of shear along the Kunlun fault to be accommodated outside of the Tibetan Plateau. Instead, shear along the Kunlun fault is accommodated or absorbed internal to the Tibetan Plateau.

ACKNOWLEDGMENTS

We thank Kevin Furlong for early review of this manuscript, Arjun Heimsath and Jean Dixon for their help in sample preparation, and Charlie Angerman for field assistance. This manuscript benefited greatly from thoughtful and thorough reviews by An Yin and Mike Oskin, and the editor, Jon Pelletier. This research was funded by National Science Foundation (NSF) grant EAR-0229955 (to Kirby) and a National Aeronautics and

Space Administration (NASA) Graduate Student Research Program (GSRP) fellowship (to Harkins).

REFERENCES CITED

Avouac, J.P., and Tapponnier, P., 1993, Kinematic model of active deformation in central Asia: Geophysical Research Letters, v. 20, p. 895–898, doi: 10.1029/93GL00128.

Barr, T.D., and Houseman, G.A., 1996, Deformation fields around a fault embedded in a non-linear ductile medium: Geophysical Journal International, v. 125, p. 473–490, doi: 10.1111/j.1365-246X.1996.tb00012.x.

Berryman, K.R., 1993, Distribution, age, and deformation of late Pleistocene marine terraces at Mahia Peninsula, Hikurangi subduction margin, New Zealand: Tectonics, v. 12, p. 1365–1379, doi: 10.1029/93TC01543.

Brown, E.T., Bendick, R., Bourles, D.L., Gaur, V., Molnar, P., Raisbeck, G.M., and Yiou, F., 2002, Slip rates of the Karakorum fault, Ladakh, India, determined using cosmic ray exposure dating of debris flows and moraines: Journal of Geophysical Research, v. 107, no. B9, 2192, doi: 10.1029/2000JB000100.

Bull, W.B., 1991, Geomorphic Response to Climate Change: New York, Oxford Press, 326 p.

Burchfiel, B.C., Deng, Q., Molnar, P., Royden, L.H., Wang, Y., Zhang, P., and Zhang, W., 1989, Intracrustal detachments within zones of intracontinental deformation: Geology, v. 17, p. 748–752, doi: 10.1130/0091-7613(1989)017<0448:IDWZOC>2.3.CO;2.

Burchfiel, B.C., Royden, L.H., van der Hilst, R.D., Hager, B.H., Chen, Z., King, R.W., Li, C., Lu, J., Yao, H., and Kirby, E., 2008, A geological and geophysical context for the Wenchuan earthquake of 12 May 2008, Sichuan, People's Republic of China: GSA Today, v. 18, no. 7, p. 4–11, doi: 10.1130/GSATG18A.1.

Chen, W.-P., and Yang, Z., 2004, Earthquakes beneath the Himalayas and Tibet: Evidence for strong lithospheric mantle: Science, v. 304, p. 1949–1956, doi: 10.1126/science.1097324.

Chevalier, M.-L., Ryerson, F.J., Tapponnier, P., Finkel, R.C., Van der Woerd, J., Li, H., and Liu, Q., 2005, Slip-rate measurements on the Karakorum fault may imply secular variations in fault motion: Science, v. 307, p. 411–414, doi: 10.1126/science.1105466.

Cowgill, E., 2007, Impact of riser reconstruction on estimation of secular variation in rates of strike-slip faulting: Revisiting the Cherchen River site along the Altyn Tagh fault, NW China: Earth and Planetary Science Letters, v. 254, no. 3–4, p. 239–255, doi: 10.1016/j.epsl.2006.09.015.

Cowgill, E., Arrowsmith, J.R., Yin, A., Xiaofeng, W., and Zhengle, C., 2004, The Akato Bend along the Altyn Tagh fault, northwest Tibet: 2. Active deformation and the importance of transpression and strain hardening within the Altyn Tagh system: Geological Society of America Bulletin, v. 116, p. 1443–1464, doi: 10.1130/B25360.1.

Cowie, P.A., and Scholz, C.H., 1992, Displacement-length scaling relationship for faults: Data synthesis and discussion: Journal of Structural Geology, v. 14, p. 1149–1156, doi: 10.1016/0191-8141(92)90066-6.

Cowie, P.A., Roberts, G.P., and Mortimer, E., 2007, Strain localisation with fault arrays over timescales of 10^0 to 10^7 years—Observations, explanations and debates, *in* Handy, M.R., Hirth, G., and Hovius, N., eds., Tectonic Faults: Agents of Change on a Dynamic Earth: Dahlem Workshop Report 95: Cambridge, Massachusetts, Massachusetts Institute of Technology (MIT) Press, p. 47–77.

Dewey, J.F., Shackleton, R.M., Chengfa, C., and Yiyin, S., 1988, The tectonic evolution of the Tibetan Plateau: Philosophical Transactions of the Royal Society London A, v. 327, p. 379–413, doi: 10.1098/rsta.1988.0135.

England, P., and McKenzie, D., 1982, A thin viscous sheet model for continental deformation: Geophysical Journal of the Royal Astronomical Society, v. 70, p. 295–321.

England, P.C., and Molnar, P., 1990, Right-lateral shear and rotation as the explanation for strike-slip faulting in eastern Tibet: Nature, v. 344, p. 140–142, doi: 10.1038/344140a0.

Fitch, T.J., 1970, Earthquake mechanisms in the Himalayan, Burmese, and Adaman regions and continental tectonics in central Asia: Journal of Geophysical Research, v. 75, p. 2699–2709, doi: 10.1029/JB075i014p02699.

Fu, B., and Awata, Y., 2007, Displacement and timing of left-lateral faulting in the Kunlun fault zone, northern Tibet, inferred from geologic and geomorphic features: Journal of Asian Earth Sciences, v. 29, p. 253–265, doi: 10.1016/j.jseaes.2006.03.004.

Gasse, F., Arnold, M., Fontes, J.C., Fort, M., Gilbert, E., Huc, A., Bingyan, L., Yuanfang, L., Qing, L., Melieres, F., Van Campo, E., Fubao, W., and Qingsong, Z., 1991, A 13,000-year climate record from western Tibet: Nature, v. 353, p. 742–745, doi: 10.1038/353742a0.

Gold, R.D., Cowgill, E., Arrowsmith, J.R., Gosse, J., Chen, X., and Wang, X.-F., 2009, Riser diachroneity, lateral erosion, and uncertainty in rates of strike-slip faulting: A case study from Tuzidun along the Altyn Tagh fault, NW China: Journal of Geophysical Research, v. 114, no. B4, B04401, doi: 10.1029/2008JB005913.

Gosse, J.C., and Phillips, F.M., 2001, Terrestrial in-situ cosmogenic nuclides: Theory and application: Quaternary Science Reviews, v. 20, p. 1475–1560, doi: 10.1016/S0277-3791(00)00171-2.

Grapes, R., Berryman, K.R., and Van Dissen, R.J., 1993, Terrace correlation, dextral displacements, and slip rate along the Wellington fault, North Island, New Zealand: Discussion and reply: New Zealand Journal of Geology and Geophysics, v. 36, no. 1, p. 131–135.

Gupta, A., and Scholz, C.H., 2000, A model of normal fault interaction based on observations and theory: Journal of Structural Geology, v. 22, p. 865–879, doi: 10.1016/S0191-8141(00)00011-0.

Gupta, S., Cowie, P.A., Dawers, N.H., and Underhill, J.R., 1998, A mechanism to explain rift-basin subsidence and stratigraphic patterns through fault-array evolution: Geology, v. 26, p. 595–598; doi: 10.1130/0091-7613(1998)026<0595:AMTERB>2.3.CO;2.

Harkins, N., and Kirby, E., 2008, Fluvial terrace riser degradation and determination of slip rates on strike-slip faults: An example from the Kunlun fault, China: Geophysical Research Letters, v. 35, L05406, doi: 10.1029/2007GL033073.

Harkins, N., Kirby, E., Heimsath, A., Robinson, R., and Reiser, U., 2007, Transient fluvial incision in the headwaters of the Yellow River, northeastern Tibet, China: Journal of Geophysical Research, v. 112, F03S04, doi: 10.1029/2006JF000570.

Hilley, G.E., Johnson, K.M., Wang, M., Shen, Z.-K., and Burgmann, R., 2009, Earthquake-cycle deformation and fault slip rates in northern Tibet: Geology, v. 37, p. 31–34, doi: 10.1130/G25157A.1.

Houseman, G., and England, P., 1993, Crustal thickening versus lateral expulsion in the Indian-Asian continental collision: Journal of Geophysical Research, v. 98, p. 12,233–12,249, doi: 10.1029/93JB00443.

Jolivet, M., Brunel, M., Seward, D., Xu, Z., Yang, J., Malavieille, J., Roger, F., Leyreloup, A., Arnaud, N., and Wu, C., 2003, Neogene extension and volcanism in the Kunlun fault zone, northern Tibet: New constraints on the age of the Kunlun fault: Tectonics, v. 22, 1052, doi: 10.1029/2002TC001428.

Kidd, W.S.F., and Molnar, P., 1988, Quaternary and active faulting observed on the 1985 Academia Sinica–Royal Society Geotraverse of Tibet: Philosophical Transactions of the Royal Society of London, v. 327, p. 337–363.

Kirby, E., Harkins, N., Wang, E., Shi, X., Fan, C., and Burbank, D., 2007, Slip rate gradients along the eastern Kunlun fault: Tectonics, v. 26, TC2010, doi: 10.1029/2006TC002033.

Knuepher, P.L.K., Bamberger, M.J., Turko, J.M., and Coppersmith, K.J., 1987, Characteristics of the boundaries of historical surface fault ruptures: Seismological Research Letters, v. 58, no. 1, p. 31.

Lal, D., 1991, Cosmic ray labeling of erosion surfaces: In-situ nuclide production rates and erosion models: Earth and Planetary Science Letters, v. 104, p. 424–439, doi: 10.1016/0012-821X(91)90220-C.

Lasserre, C., Morel, P.H., Gaudemer, Y., Tapponnier, P., Ryerson, F.J., King, G., Metivier, F., Kasser, M., Kashgarian, M., Liu, B., Lu, T., and Yuan, D., 1999, Postglacial left slip rate and past occurrence of M> or =8 earthquakes on the western Haiyuan fault, Gansu, China: Journal of Geophysical Research, v. 104, no. B8, p. 17,633–17,652, doi: 10.1029/1998JB900082.

Lasserre, C., Gaudemer, Y., Tapponnier, P., Meriaux, A., Van der Woerd, J., Daoyang, Y., Ryerson, F.J., Finkel, R., and Caffee, M., 2002, Fast late Pleistocene slip rate on the Leng Long Ling segment of the Haiyuan fault, Qinghai, China: Journal of Geophysical Research, v. 107, no. B11, 2276, doi: 10.1029/2000JB000060.

Lasserre, C., Peltzer, G., Crampé, F., Klinger, Y., Van der Woerd, J., and Tapponnier, P., 2005, Coseismic deformation of the 2001 M_w = 7.8 Kokoxili earthquake in Tibet, measured by synthetic aperture radar interferometry: Journal of Geophysical Research, v. 110, B12408, doi: 10.1029/2004JB003500.

Lawn, B.R., 1975, Fracture of Brittle Solids: Cambridge, UK, Cambridge University Press, 400 p.

Lensen, G.J., 1964a, The faulted terrace sequence at the Grey River, Awatere Valley, South Island, New Zealand: New Zealand Journal of Geology and Geophysics, v. 7, p. 871–876.

Lensen, G.J., 1964b, The general case of progressive fault displacement of flights of degradational terraces: New Zealand Journal of Geology and Geophysics, v. 7, p. 864–870.

Li, H., and Jia, Y., 1981, Characteristics of the deformation band of the 1937 Tuosuohu earthquake (M=7.5) in Qinghai: Northwestern Seismological Journal, v. 3, p. 61–65.

Li, H., Van der Woerd, J., Tapponnier, P., Klinger, Y., Qi, X., Yang, J., and Zhu, Y., 2005, Slip rate on the Kunlun fault at Hongshui Gou, and recurrence time of great events comparable to the 14/11/2001, Mw~7.9 Kokoxili earthquake: Earth and Planetary Science Letters, v. 237, p. 285–299, doi: 10.1016/j.epsl.2005.05.041.

Lin, A., and Guo, J., 2008, Nonuniform slip rate and millennial recurrence interval of large earthquakes along the eastern segment of the Kunlun fault, northern Tibet: Bulletin of the Seismological Society of America, v. 98, p. 2866–2878, doi: 10.1785/0120070193.

Lin, A., Fu, B., Guo, J., Zeng, Q., Dang, G., He, W., and Zhao, Y., 2002, Co-seismic strike-slip and rupture length produced by the 2001 Ms 8.1 central Kunlun earthquake: Science, v. 296, no. 5575, p. 2015–2017, doi: 10.1126/science.1070879.

Meade, B.J., 2007, Present-day kinematics at the India-Asia collision zone: Geology, v. 35, p. 81–84, doi: 10.1130/G22924A.1.

Mériaux, A.-S., Ryerson, F.J., Tapponnier, P., Van der Woerd, J., Finkel, R.C., Xu, X., Xu, Z., and Caffee, M.W., 2004, Rapid slip along the central Altyn Tagh fault: Morphochronologic evidence from Cherchen He and Sulamu Tagh: Journal of Geophysical Research, v. 109, B06401, doi: 10.1029/2003JB002558.

Mériaux, A.-S., Tapponnier, P., Ryerson, F.J., Xu, X., King, G., Van der Woerd, J., Finkel, R.C., Li, H., Caffee, M.W., Xu, Z., and Chen, W., 2005, The Aksay segment of the northern Altyn Tagh fault: Tectonic geomorphology, landscape evolution, and Holocene slip rate: Journal of Geophysical Research, v. 110, B04404, doi: 10.1029/2004JB003210.

Molnar, P., and Lyon-Caen, H., 1989, Fault plane solutions of earthquakes and active tectonics of the Tibetan Plateau and its margins: Geophysical Journal International, v. 99, p. 123–153, doi: 10.1111/j.1365-246X.1989.tb02020.x.

Molnar, P., and Tapponnier, P., 1975, Cenozoic tectonics of Asia: Effects of a continental collision: Science, v. 189, p. 419–426, doi: 10.1126/science.189.4201.419.

Murphy, M.A., Yin, A., Kapp, P., Harrison, T.M., Lin, D., and Jinghui, G., 2000, Southward propagation of the Karakoram fault system, southwest Tibet: Timing and magnitude of slip: Geology, v. 28, p. 451–454, doi: 10.1130/0091-7613(2000)28<451:SPOTKF>2.0.CO;2.

Owen, L.A., Finkel, R., Haizhou, M., Spencer, J.Q., Derbyshire, E., Barnard, P.L., and Caffee, M., 2003, Timing and style of late Quaternary glaciation in northeastern Tibet: Geological Society of America Bulletin, v. 115, p. 1356–1364, doi: 10.1130/B25314.1.

Peltzer, G., and Saucier, F., 1996, Present-day kinematics of Asia derived from geologic fault rates: Journal of Geophysical Research, v. 101, p. 27,943–27,956, doi: 10.1029/96JB02698.

Peltzer, G., Tapponnier, P., Zhang, Z., and Xu, Z., 1985, Neogene and Quaternary faulting in and along the Qinling Shan: Nature, v. 317, p. 500–505, doi: 10.1038/317500a0.

Peltzer, G., Crampé, F., and King, G., 1999, Evidence of nonlinear elasticity of the crust from the Mw 7.6 Manyi (Tibet) earthquake: Science, v. 286, p. 272–276, doi: 10.1126/science.286.5438.272.

Phillips, F.M., Zreda, M., Gosse, J.C., Klein, J., Evenson, E.B., Hall, R.D., Chadwick, O.A., and Sharma, P., 1997, Cosmogenic ^{36}Cl and ^{10}Be ages of Quaternary glacial and fluvial deposits of the Wind River Range, Wyoming: Geological Society of America Bulletin, v. 109, p. 1453–1463, doi: 10.1130/0016-7606(1997)109<1453:CCABAO>2.3.CO;2.

Poisson, B., and Avouac, J.-P., 2004, Holocene hydrological changes inferred from alluvial stream entrenchment in North Tian Shan (northwestern China): The Journal of Geology, v. 112, p. 231–249, doi: 10.1086/381659.

Putkonen, J., and O'Neal, M., 2006, Degradation of unconsolidated Quaternary landforms in western North America: Geomorphology, v. 75, no. 3–4, p. 408–419, doi: 10.1016/j.geomorph.2005.07.024.

Roberts, G.P., and Michetti, A.M., 2004, Spatial and temporal variations in growth rates along active normal fault systems: An example from Lazio-Abruzzo, central Italy: Journal of Structural Geology, v. 26, p. 339–376, doi: 10.1016/S0191-8141(03)00103-2.

Robinson, A.C., 2009, Geologic offsets across the northern Karakorum fault: Implications for its role and terrane correlations in the western Himalayan-Tibetan orogen: Earth and Planetary Science Letters, v. 279, p. 123–130, doi: 10.1016/j.epsl.2008.12.039.

Ruddiman, W.F., and Kutzbach, J.E., 1989, Forcing of late Cenozoic Northern Hemisphere climate by plateau uplift in southern Asia and the American West: Journal of Geophysical Research, v. 94, no. D15, p. 18,409–18,427, doi: 10.1029/JD094iD15p18409.

Schlische, R.W., Young, S.S., Ackerman, R.V., and Gupta, A., 1996, Geometry and scaling relations of a population of very small rift-related normal faults: Geology, v. 24, p. 683–686, doi: 10.1130/0091-7613(1996)024<0683:GASROA>2.3.CO;2.

Shen, Z.-K., Lü, J., Wang, M., and Bürgmann, R., 2005, Contemporary crustal deformation around the southeast borderland of the Tibetan Plateau: Journal of Geophysical Research, v. 110, B11409, doi: 10.1029/2004JB003421.

Stirling, M.W., Wesnousky, S.G., and Shimazaki, K., 1996, Fault trace complexity, cumulative slip, and the shape of the magnitude-frequency distribution for strike-slip faults: A global survey: Geophysical Journal International, v. 124, p. 833–868, doi: 10.1111/j.1365-246X.1996.tb05641.x.

Stone, J.O., 2000, Air pressure and cosmogenic isotope production: Journal of Geophysical Research, v. 105, p. 23,753–23,759, doi: 10.1029/2000JB900181.

Stuiver, M., Reimer, P.J., Bard, E., Beck, J.W., Burr, G.S., Hughen, K.A., Kromer, B., McCormac, G., Van Der Plicht, J., and Spurk, M., 1998, INTCAL98 Radiocarbon age calibration 24,000–0 cal BP: Radiocarbon, v. 40, p. 1041–1083.

Tapponnier, P., and Molnar, P., 1977, Active faulting and tectonics in China: Journal of Geophysical Research, v. 82, p. 2905–2930, doi: 10.1029/JB082i020p02905.

Tapponnier, P., Peltzer, G., Le Dain, A.Y., Armijo, R., and Cobbold, P., 1982, Propagating extrusion tectonics in Asia: New insight from simple experiments with plasticine: Geology, v. 10, p. 611–616, doi: 10.1130/0091-7613(1982)10<611:PETIAN>2.0.CO;2.

Tapponnier, P., Meyer, B., Avouac, J.-P., Gaudemer, Y., Peltzer, G., Guo, S., Xiang, H., Yin, K., Chen, Z., Cai, S., and Dai, H., 1990, Active thrusting and folding in the Qi Lian Shan, and decoupling between the upper crust and mantle in northeastern Tibet: Earth and Planetary Science Letters, v. 97, p. 382–403, doi: 10.1016/0012-821X(90)90053-Z.

Tapponnier, P., Zhiqin, X., Roger, F., Meyer, B., Arnaud, N., Wittlinger, G., and Jingsui, Y., 2001, Oblique stepwise rise and growth of the Tibet Plateau: Science, v. 294, p. 1671–1677, doi: 10.1126/science.105978.

Thatcher, W., 2007, Microplate model for the present-day deformation of Tibet: Journal of Geophysical Research, v. 112, B01401, doi: 10.1029/2005JB004244.

Thompson, L.G., Yao, Y., Davis, M.E., Henderson, K.A., Mosely-Thompson, E., Lin, P.N., Beer, J., Synal, H.A., Cole-Dai, J., and Bolzan, J.F., 1997, Tropical climate instability; the last glacial cycle from the Qinghai-Tibetan ice core: Science, v. 276, no. 5320, p. 1821–1825, doi: 10.1126/science.276.5320.1821.

Van der Woerd, J., Ryerson, F.J., Tapponnier, P., Gaudemer, Y., Finkel, R., Meriaux, A.S., Caffee, M., Zhao, G., and He, Q., 1998, Holocene left-slip rate determined by cosmogenic surface dating on the Xidatan segment of the Kunlun fault (Qinghai, China): Geology, v. 26, p. 695–698, doi: 10.1130/0091-7613(1998)026<0695:HLSRDB>2.3.CO;2.

Van der Woerd, J., Ryerson, F.J., Tapponnier, P., Meriaux, A.-S., Gaudemer, Y., Meyer, B., Finkel, R.C., Caffee, M.W., Zhao, G., and Xu, Z., 2000, Uniform slip-rate along the Kunlun Fault: Implications for seismic behavior and large-scale tectonics: Geophysical Research Letters, v. 27, p. 2353–2356, doi: 10.1029/1999GL011292.

Van der Woerd, J., Meriaux, A.-S., Klinger, Y., Ryerson, F.J., Gaudemer, Y., and Tapponnier, P., 2002a, The 14 November 2001, Mw=7.8 Kokoxili earthquake in northern Tibet (Qinghai Province, China): Seismological Research Letters, v. 73, no. 2, p. 125–135.

Van der Woerd, J., Tapponnier, P., Ryerson, F.J., Meriaux, A.-S., Meyer, B., Gaudemer, Y., Finkel, R.C., Caffee, M.W., Zhao, G., and Xu, Z., 2002b, Uniform postglacial slip-rate along the central 600 km of the Kunlun fault (Tibet), from ^{26}Al, ^{10}Be, and ^{14}C dating of riser offsets, and climatic origin of the regional morphology: Geophysical Journal International, v. 148, p. 356–388, doi: 10.1046/j.1365-246x.2002.01556.x.

Walsh, J.J., Nicol, A., and Childs, C., 2002, An alternative model for the growth of faults: Journal of Structural Geology, v. 24, p. 1669–1675, doi: 10.1016/S0191-8141(01)00165-1.

Wang, Q., Zhang, P., Freymueller, J.T., Bilham, R., Larson, K., Lai, X., You, X., Niu, Z., Wu, J., Li, Y., Liu, J., Yang, Z., and Chen, Q., 2001, Present-day crustal deformation in China constrained by global positioning system measurements: Science, v. 294, p. 574–577, doi: 10.1126/science.1063647.

Wesnousky, S.G., 1988, Seismological and structural evolution of strike-slip faults: Nature, v. 355, p. 340–343, doi: 10.1038/335340a0.

Yin, A., 2000, Mode of Cenozoic east-west extension in Tibet suggesting a common origin of rifts in Asia during the Indo-Asian collision: Journal of Geophysical Research, v. 105, no. B9, p. 21,745–21,759, doi: 10.1029/2000JB900168.

Yin, A., and Harrison, T.M., 2000, Geologic evolution of the Himalayan-Tibetan orogen: Annual Review of Earth and Planetary Sciences, v. 28, p. 211–280, doi: 10.1146/annurev.earth.28.1.211.

Yin, A., Dang, Y., Zhang, M., McRivette, M.W., Burgess, W.P., and Chen, X., 2007, Cenozoic tectonic evolution of Qaidam Basin and its surrounding regions: Part 2. Wedge tectonics in southern Qaidam Basin and the Eastern Kunlun Range, *in* Sears, J.W., Harms, T.A., and Evenchick, C.A., eds., Whence the Mountains? Inquiries into the Evolution of Orogenic Systems: A Volume in Honor of Raymond A. Price: Geological Society of America Special Paper 433, p. 369–390, doi: 10.1130/2007.2433(18).

Yin, A., Dang, Y., Zhang, M., Chen, X., and McRivette, M.W., 2008, Cenozoic tectonic evolution of the Qaidam Basin and its surrounding regions: Part 3. Structural geology, sedimentation, and regional tectonic reconstruction: Geological Society of America Bulletin, v. 120, p. 847–876, doi: 10.1130/B26232.1.

Yuan, D., Lei, Z.-S., Wen-Gui, H., Xiong, Z., Ge, W.-P., Liu, X.-W., and Liu, B.-C., 2007, Textural research of the Wudu earthquake in 186 B.C. in Gansu Province, China, and discussion on its causative structure: Acta Seismologic Sinica (English version), v. 20, no. 6, p. 696–707, doi: 10.1007/s11589-007-0696-5.

Zhang, P., and Molnar, P., 2007, Late Quaternary and present-day rates of slip along the Altyn Tagh fault, northern margin of the Tibetan Plateau: Tectonics, v. 26, no. 5, TC5010, doi: 10.1029/2006TC002014.

Zhang, P., Ellis, M., Slemmons, D.B., and Mao, F., 1990, Right-lateral displacements and the Holocene slip rate associated with prehistoric earthquakes along the southern Panamint Valley fault zone: Implications for southern Basin and Range tectonics and coastal California deformation: Journal of Geophysical Research, v. 95, p. 4857–4872, doi: 10.1029/JB095iB04p04857.

Zhang, P.-Z., Shen, Z.-K., Wang, M., Gan, W., Burgmann, R., Molnar, P., Wang, Q., Niu, Z., Sun, J., Wu, J., Hanrong, S., and Xinzhao, Y., 2004, Continuous deformation of the Tibetan Plateau from global positioning system data: Geology, v. 32, p. 809–812, doi: 10.1130/G20554.1.

Zhang, Y.Q., Mercier, J.L., and Vergély, P., 1998, Extension in the graben systems around the Ordos (China), and its contribution to the extrusion tectonics of south China with respect to Gobi-Mongolia: Tectonophysics, v. 285, p. 41–75, doi: 10.1016/S0040-1951(97)00170-4.

Zhou, D., and Graham, S.A., 1996, Songpan-Ganzi complex of the west Qilian Shan as a Triassic remnant ocean basin, *in* Yin, A., and Harrison, T. M., eds., The Tectonic Evolution of Asia: Cambridge, UK, Cambridge University Press, p. 281–299.

MANUSCRIPT RECEIVED 1 NOVEMBER 2009
REVISED MANUSCRIPT RECEIVED 18 APRIL 2010
MANUSCRIPT ACCEPTED 18 MAY 2010

Printed in the USA